

## Article

# Small molecule inhibitors of KDM5 histone demethylases increase radio-sensitivity of breast cancer cells over-expressing JARID1B

Simone Pippa<sup>1</sup>, Cecilia Mannironi<sup>2</sup>, Valerio Licursi<sup>3</sup>, Luca Bombardi<sup>1</sup>, Gianni Colotti<sup>2</sup>, Enrico Cundari<sup>2</sup>, Adriano Mollica<sup>4</sup>, Antonio Coluccia<sup>5</sup>, Valentina Naccarato<sup>5</sup>, Giuseppe La Regina<sup>5</sup>, Romano Silvestri<sup>5</sup> and Rodolfo Negri<sup>1,2\*</sup>

<sup>1</sup> Dipartimento di Biologia e Biotecnologie C. Darwin, Sapienza Università di Roma, Rome, Italy; [simone.pippa@uniroma1.it](mailto:simone.pippa@uniroma1.it) (S.P.); [luca.bombardi@uniroma1.it](mailto:luca.bombardi@uniroma1.it) (LB); [rodolfo.negri@uniroma1.it](mailto:rodolfo.negri@uniroma1.it) (R.N.)

<sup>2</sup> Istituto di Biologia e Patologia Molecolari, Consiglio Nazionale delle Ricerche, Rome, Italy; [cecilia.mannironi@uniroma1.it](mailto:cecilia.mannironi@uniroma1.it) (C.M.); [gianni.colotti@uniroma1.it](mailto:gianni.colotti@uniroma1.it) (G.C.); [enrico.cundari@uniroma1.it](mailto:enrico.cundari@uniroma1.it) (E.C.);

<sup>3</sup> Istituto di Analisi dei Sistemi ed Informatica “Antonio Ruberti”, Consiglio Nazionale delle Ricerche, Rome, Italy; [valerio.licursi@uniroma1.it](mailto:valerio.licursi@uniroma1.it) (V.L.);

<sup>4</sup> Dipartimento di Farmacia, Università di Chieti-Pescara «G. D’Annunzio», Via dei Vestini 31, 66100 Chieti, Italy, [adriano.mollica@unich.it](mailto:adriano.mollica@unich.it) (A.M.)

<sup>5</sup> Dipartimento di Chimica e Tecnologie del Farmaco, Laboratory affiliated to Istituto Pasteur Italia - Fondazione Cenci Bolognetti, Sapienza Università di Roma, Rome, Italy; [antonio.coluccia@uniroma1.it](mailto:antonio.coluccia@uniroma1.it) (A.C.); [valentina.naccarato@uniroma1.it](mailto:valentina.naccarato@uniroma1.it) (V.N.); [giuseppe.laregina@uniroma1.it](mailto:giuseppe.laregina@uniroma1.it) (G.L.R.); [romano.silvestri@uniroma1.it](mailto:romano.silvestri@uniroma1.it) (R.S.);

\* Correspondence: [rodolfo.negri@uniroma1.it](mailto:rodolfo.negri@uniroma1.it); Tel.: +39-06-4991-7790

† These authors contributed equally to this work.

## Abstract:

**Background:** KDM5 enzymes are H3K4 specific histone demethylases involved in transcriptional regulation and DNA repair. These proteins are over-expressed in different kinds of cancer, including breast, prostate and bladder carcinoma, with positive effects on cancer proliferation and chemo-resistance. For these reasons, these enzymes are potential therapeutic cancer targets.

**Methods:** In the present study, we analyzed the effects of three different inhibitors of KDM5 enzymes in MCF-7 breast cancer cells over-expressing JARID1B. In particular we tested H3K4 demethylation (western blot); target gene transcription (RNAseq and real time PCR); radio-sensitivity (citotoxicity and clonogenic assays) and damage accumulation (kinetics of H2AX phosphorylation).

**Results:** we show that two compounds with completely different chemical structure can selectively inhibit KDM5 enzymes and that both compounds are capable of increasing sensitivity of breast cancer cells to ionizing radiation and H2AX phosphorylation.

**Conclusions:** These findings confirm the involvement of H3K4 specific demethylases in DNA damage signaling and repair and suggest new strategies for the therapeutic use of their inhibitors.

**Keywords:** Histone demethylase inhibitors, DNA damage, epigenetic drugs, breast cancer.

## 1. Introduction

Histone lysine methylation is a post-translational modification that influences many aspects of cell biology, such as transcription, epigenetic inheritance, nuclear architecture and genome stability [1-2]. Unlike histone acetylation, histone methylation may lead either to transcriptional repression or activation, depending on which residue is involved [3]. Due to the importance of this epigenetic mark, a tight regulation of histone methylation has been evolved. The enzymes capable of erasing methyl groups from histones are the histone lysine demethylase (KDMs) and in human these enzymes are represented by two families of proteins: the Lysine Specific histone Demethylase (LSD) family and the JmjC domain- containing family also known as the Jumonji Histone Demethylases (JHDMs) [4-7]. These two families differ in their catalytic mechanisms. The LSD KDMs are monoamine oxidases whereas JHDMs are hydroxylases that require two cofactors for their function, Fe(II) and 2-oxoglutarate, which are bound in the JmjC catalytic domain. Among the latter ones, particularly interesting are those using H3K4me2 and H3K4me3 as substrates, the KDM5 (or JARID1) enzymes. H3K4 methylation seems to play an important role in development and differentiation and transcriptional regulation [8-9]. Indeed, actively transcribed genes have promoters often marked with H3K4 tri-methylation [10]. Therefore, at first glance, KDM5 enzymes seem to act as transcriptional repressors but, recently, it has been proposed that KDM5 demethylases could also remove tri- and di- methyl groups at enhancer regions. Since H3K4me1 modification combined with acetylated H3K27 (H3K27ac) is predictive of active enhancers, KDM5 enzymes could also have a role in transcription activation [11]. KDM5 subfamily (also known as JARID1 subfamily) consists of four members, KDM5A (JARID1A), KDM5B (JARID1B), KDM5C (JARID1C) and KDM5D (JARID1D) whose deregulation in various kinds of cancer has been widely documented to contribute significantly to tumor initiation and progression [12-16]. Indeed, KDM5B was initially identified as a gene markedly over-expressed in breast cancer even before the discovery of histone lysine demethylases [14]. Nevertheless, it was later observed that the deregulation of this protein is different among the different breast cancer subtypes, thus suggesting a crucial but ambivalent role for KDM5B depending on the cell type context [17]. Later, it was also found to be over-expressed in prostate, lung and bladder carcinoma [13,15]. In the same way, KDM5A was first named RBP2 because it was found to be associated with the master tumor suppressor pRb [18]. By inhibiting pRb activity, KDM5A appears to be a positive regulator of proliferation [19], and it was, in fact, observed to be upregulated in gastric [16] and cervical carcinoma [20]. Recent evidences suggest that KDMC promotes tumor cells migration and invasion in breast cancer [21].

As regard the outcome of the action of these proteins on transcription, KDM5B interacts with Cdh4 (a member of NuRD complex) and HDAC1 [22]. The cooperative action resulting by the association of these three catalytic proteins provides a powerful mechanism for a rapid repression of actively transcribed genes involving H3K4 demethylation, lysine deacetylation, and ATPase-mediated chromatin remodeling.

Beside the role in transcriptional regulation, new findings suggest that KDM5 members are involved in the mechanisms of maintenance of genomic stability. KMD5B is enriched at DNA-damage sites after ionizing radiation and its demethylase activity is required for an efficient DNA repair, in contrast with previous observations suggesting a positive role for H3K4 methylation in DNA repair. An interesting model proposed by Li and colleagues [23] tries to establish a connection between the different roles of KDM5B in transcriptional regulation and in DNA repair. During transcriptional activation, PARP1 PARylates KDM5B and prevents it from demethylating H3K4 which would result in shutting off transcription. However, when chromatin is damaged, PARylated KDM5B can be recruited to the damaged sites by histone variant macroH2A1.1 thanks to its PAR binding domain. Local H3K4 demethylation performed by KDM5B is essential for Ku70/80 and BRCA1 recruitment, in NHEJ and HR pathways, respectively. Moreover, Li and colleagues observed an enhanced and prolonged phosphorylation of H2AX and p53 when cells lacking KDM5B are irradiated and the phosphorylation of these two key players in DNA Damage Repair (DDR) occurs also in non-irradiated cells, suggesting a crucial role for KDM5B as in genome's integrity surveillance, regardless of irradiation. A similar mechanism has been recently proposed for KDM5A

as well, even though it is still not clear whether the catalytic activity of this enzyme is necessary for DNA repair or in this case the stimulation of repair is achieved by an indirect mechanism [24].

For the pivotal functions of KDM5 enzymes in different cellular processes, it is important to understand the mechanisms underlying their regulation. Moreover, given the prominent role they have in oncogenesis, they are also promising candidate as therapeutic targets.

In the last decade, an increasing number of epigenetic inhibitors has been developed [25]. Among these, compounds targeting histone lysine demethylase are of great interest because several members of this family of enzymes play a pivotal role in diseases [26]. Thus, histone lysine demethylases are considered putative drug targets primarily because we acquired a good knowledge of their active site structure [7; 27-29]. This feature allows us to develop high-affinity inhibitors [30-32]. Small molecules that can regulate site-specific methylation can be used both as chemical tools for studying the function of the epigenetic modifiers and as candidate therapeutic agents for diseases caused by aberrant histone methylation [33-34].

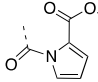
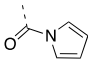
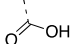
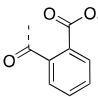
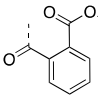
Some inhibitors of KDM5 subfamily of JHDMs have been developed [33-38]. Since the catalytic mechanism of these proteins relies on  $\alpha$ -ketoglutarate, the inhibitors for JHDMs are mostly compounds mimicking this cofactor [39-40], with very few exceptions [28].

## 2. Results

### 2.1. RS 3195 is a KDM5 enzymes inhibitor that induces a strong G2/M arrest in MCF-7 cells

We previously set up an *in vivo* screening system to select H3K4-Specific Histone Demethylase inhibitors which allowed us to find a new potential inhibitor of KDM5 enzymes, starting from a library of about 6000 compounds predicted to mimic the structure of  $\alpha$ -ketoglutarate [36]. The molecule identified, called RS 3195 is shown in Table 1. Further analysis showed that this compound was able to selectively inhibit KDM5B and KDM5D activity *in vitro* and to decrease H3K4 demethylation in HeLa cells without affecting other lysines methylation [36]. Since we were particularly interested to the role of KDM5 enzymes in oncogenesis and transcriptional regulation, we decided to focus our analysis on the effects of our compound on MCF-7 breast cancer cell line in which KDM5B over-expression is a crucial feature because it has wide effects on proliferation, transcription regulation and drug resistance [41]. To assess the ability of RS 3195 to inhibit KDM5 enzymes, we treated MCF-7 cells with three different concentrations of inhibitor (1  $\mu$ M, 10  $\mu$ M and 30  $\mu$ M). Since in human the only enzymes accountable for the demethylation of tri-methylated H3K4 are KDM5 histone demethylases, we monitored the levels of H3K4me3 upon RS 3195 treatment. As previously observed in HeLa cells [36], RS 3195 induces a slight increase in H3K4me3 levels in bulk chromatin of MCF-7 as well (SM Figure 1-2), although, due to high variability, this effect is not statistically significant. However, we noticed that RS 3195 strongly affects cell cycle dynamics of MCF-7 at 30  $\mu$ M, inducing a clear increase of cells in G2/M (Figure 1A-B). No cell cycle perturbation was observed at 1  $\mu$ M and 10  $\mu$ M. A similar result was previously observed in HeLa cells [36], suggesting a cytostatic effect of this compound at higher concentrations.

**Table 1.** Chemical Structures for RS Compounds 3195, 3152, 3183, 5033 and 4995.

Compd	R <sub>1</sub>	Position	R <sub>2</sub>
RS3195	CH <sub>3</sub> O	3	
RS3152	CH <sub>3</sub> O	3	
RS3183	CH <sub>3</sub> O	3	
RS5033	CH <sub>3</sub> O	3	
RS4995	Br	4	

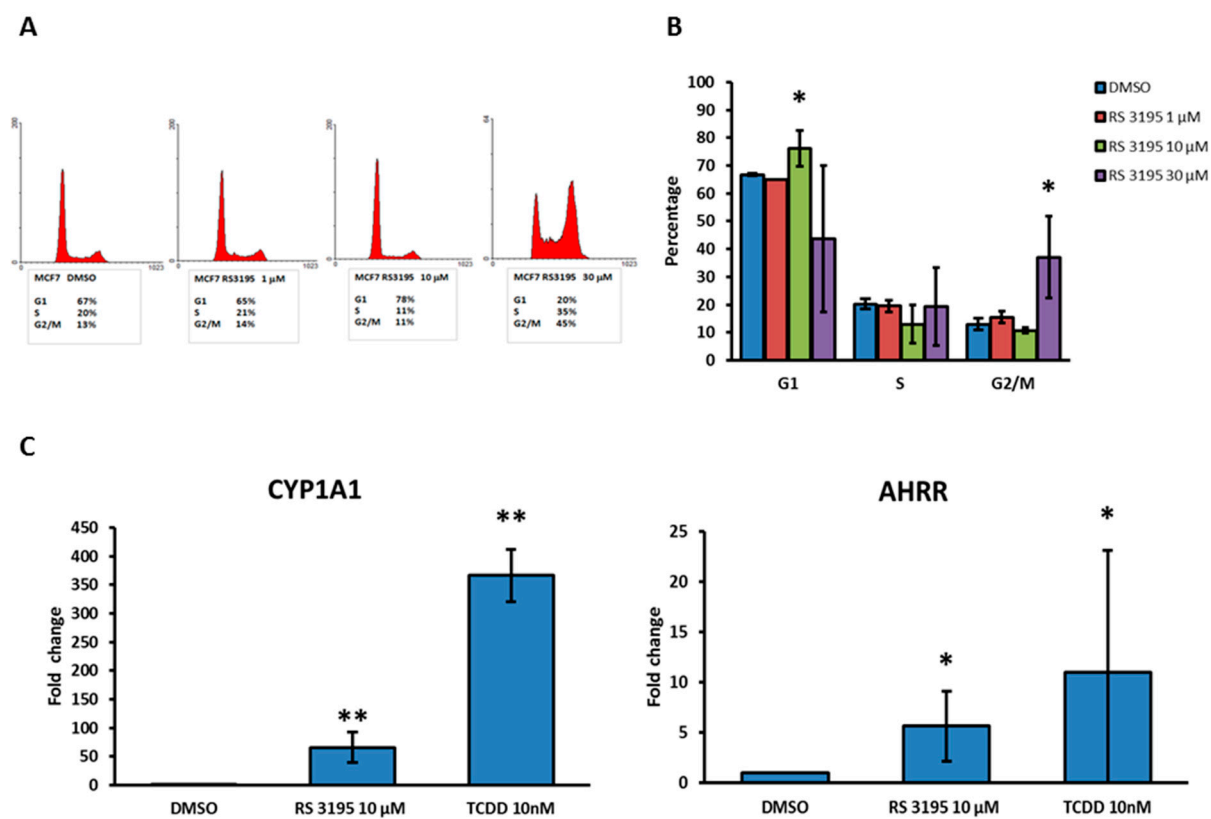


**Figure 1.** RS 3195 is a KDM5 enzymes inhibitor that induces a strong G2/M arrest in MCF-7 cells. (A) Flow-cytometry analysis of cell-cycle distribution of MCF-7 cells treated with three different concentrations of RS 3195. The image is representative of three independent experiments. (B) Quantification of three independent experiments of flow cytometry analysis, indicating a strong increase in G2/M cells upon 30  $\mu$ M RS 3195 treatment. Data are represented as the mean  $\pm$  SD of the corresponding percentage of cells in different cell cycle phases. (C) Transcript levels analysis by Real Time PCR of CYP1A1 and AHRR, in MCF-7 cells treated with 10  $\mu$ M RS 3195, indicating that this compound activates Aryl-hydrocarbon response. TCDD is used as control of the activation of AhR response as it is considered the best-known elicitor of the pathway. Data are represented as the mean  $\pm$  SD of mRNA levels fold change from four independent experiments with respect to DMSO control. Statistical significance was assessed according to two-tailed paired Student's t test. \*  $p < 0.05$ ; \*\*  $p < 0.001$ .

## 2.2. KDM5 enzymes inhibition does not significantly change the transcriptome of MCF-7 cells

To define a transcriptomic signature of H3K4 tri-methylation and dissect the role of KDM5 enzymes in transcriptional regulation and oncogenesis, we performed an RNA-seq on MCF-7 cells treated with RS 3195. To minimize the cytostatic effect of our inhibitor, we treated cells with a concentration of 10  $\mu$ M which does not significantly perturb the cell cycle dynamics. We found some genes significantly modulated upon treatment (SM Table1) but a complete functional analysis (SM figures 3-4) showed no remarkable alterations in specific gene expression patterns. This limited effect on gene transcription is in accordance with the data provided by Yamamoto and colleagues [41] who observed only modest variations of transcript levels in siKDM5B transfected breast cancer cells, especially in luminal breast cancer cells. Thus, they suggested that KDM5B is not a strong transcriptional repressor but rather a fine-tuning regulator of cell type-specific H3K4 methylation and transcript levels. However, we noticed that the top up-regulated genes (SM Table1), CYP1A1, CYP1B2, ALDH1A3 and AHRR) were all known to be involved in the aryl hydrocarbon receptor (AhR) response [42-44], a signaling pathway activated by xenobiotics, suggesting that the most significant transcriptomic changes caused by our compound could be due to its potential toxicity. We verified the activation of AhR pathway by analyzing levels of CYP1A1 and AHRR transcripts by Real Time PCR in MCF-7 cells treated with RS 3195. This analysis confirmed that RS 3195 induces the genes involved in AhR pathway even in a minor extent as compared with the main known elicitor of AhR, TCDD (Figure 1C). AhRR gene was previously shown to repress the growth of MCF-7 cells affecting transcriptional and/or posttranscriptional regulations of estrogen responsive and cell cycle-related genes [45].

## 2.3. Designing RS 5033, a selective KDM5 enzymes inhibitor with no effects on cell cycle dynamics

To gain more insight the RS3195 binding mode we performed docking experiments. The binding mode of the inhibitor was evaluated at the  $\alpha$ -KG binding pocket of the KDM5B crystal structure [46-47]. Analyses of the docking poses led us to highlight some key binding interactions: (i) the oxygen atoms of the carboxylate and of the carbonyl al position 1 of the pyrrole formed coordination contacts with the catalytic iron atom; (ii) the pyrrole nucleus formed staking interactions with the aromatic rings of the Tyr488 and Phe496; (iii) the sulfonamide oxygen atoms were involved in H-bond with Arg98; (iv) the terminal phenyl ring formed staking contacts with Trp486. (Figure 2)

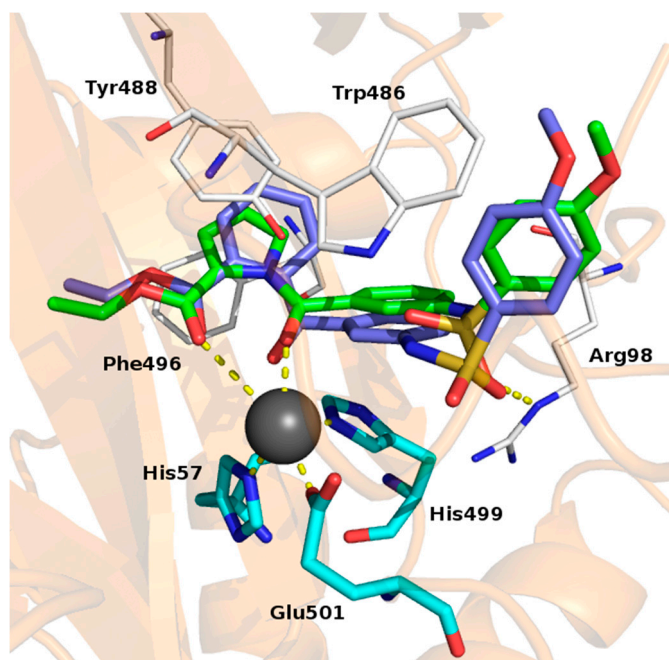


**Figure 2.** Proposed binding mode for RS3195 (green) and RS5033 (magenta). The iron atom is reported as grey sphere; the coordinating residues are depicted as cyan sticks and the coordination bond as dotted yellow lines. The residues involved in interactions with the inhibitors are reported as white lines. H-bond is reported as yellow dot lines.

A test set of RS3195 analogues was synthesized and evaluated by Surface Plasmon Resonance to confirm the proposed binding mode and to draw some structure activity relationships. Compounds lacking either the carboxylic moiety (RS 3152) or the pyrrole-2-carboxylic group (RS 3183) were predicted to be less active than RS3195. Indeed, both compounds do not possess the iron chelating moieties. We aimed to strengthen the aromatic interactions by replacing the pyrrole nucleus with a phenyl ring (RS5033). Finally, we moved the R<sub>2</sub> substituent (Table 1) from position 3 to position 4 of the central phenyl ring (RS4995). All the new compounds were evaluated by docking experiments. Worthily, derivatives RS4995 and RS5033 shared the same binding mode of RS3195, whereas RS3152 and RS3183 showed distinct binding mode.

We tested the relative affinity of these molecules for KDM5D enzyme by Surface Plasmon Resonance (SPR) at various concentrations of compounds (Figure 3; SM Figure 5) and, as predicted, RS 3152 and RS 3183 showed lower affinity for KDM5 compared to RS 3195. RS 4995 resulted to have a similar affinity whereas RS 5033 proved to be the most affine compound for the catalytic site of the enzyme.

The SPR results were in good agreement with the proposed binding modes. The experimental data highlighted the key role of the moieties that bound the catalytic iron atom.



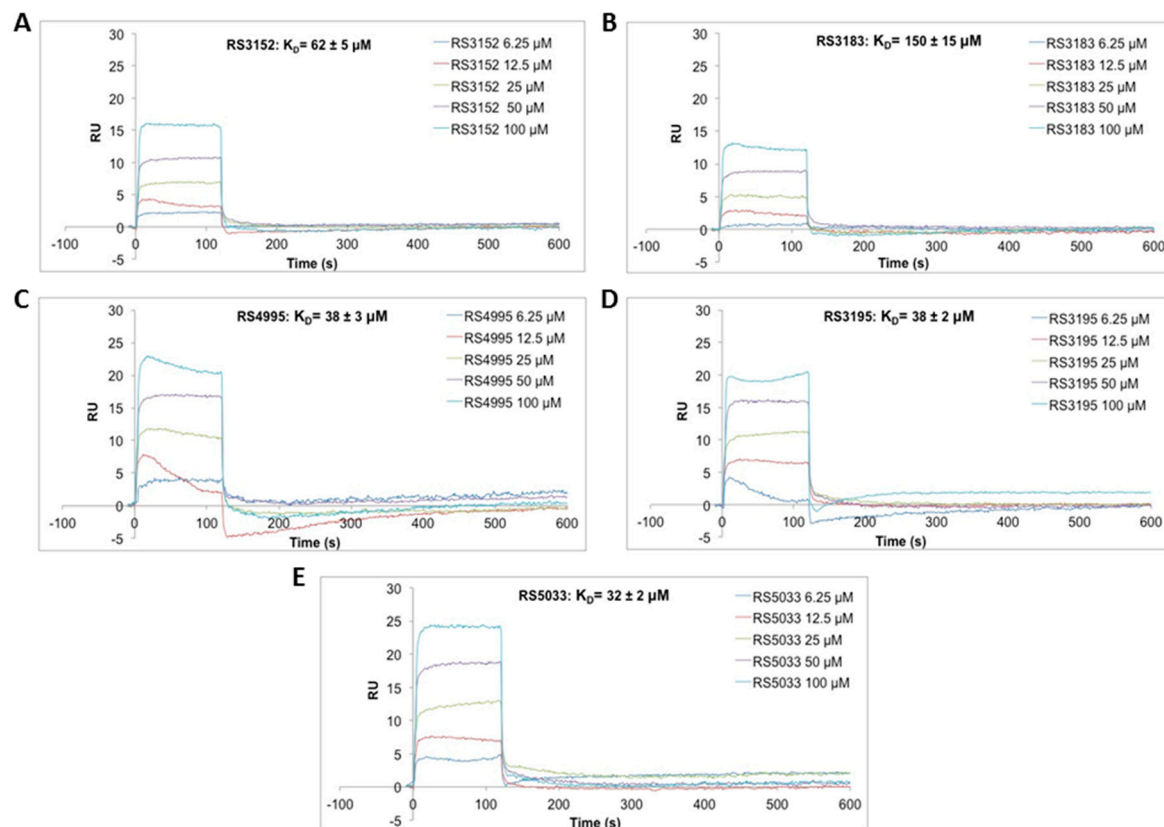


**Figure 3.** SPR sensorgrams showing the interaction of KDM5D immobilized on a COOH5 sensorchip between analytes (inhibitors RS3152, RS3183, RS3195, RS4995, RS5033 in buffer HSP-1%D) at the following concentrations: 6.25 μM; 12.5 μM; 25 μM; 50 μM; 100 μM. The increase in RU relative to baseline indicates complex formation; the plateau region represents the steady-state phase of the interaction, whereas the decrease in RU after 120 s represents dissociation of analytes from immobilized KDM5D after injection of buffer HSP-1%D.

When tested *in vitro* (see Materials and Methods) RS 5033 proved to be slightly more active than RS 3195 (Table2). Hence, we tested the *in vivo* effect of different concentration of RS 5033 (1 μM, 10 μM and 30 μM) on H3K4 tri-methylation and on the cell cycle dynamics in MCF-7 cells. Western blotting analysis on bulk chromatin demonstrated that RS 5033 induces a more remarkable and significant increase of H3K4me3 compared to RS 3195 (Figure 4A-B). Moreover, this compound does not increase H3K9 and H3K27 methylation levels, suggesting a predominant inhibitory action of RS 5033 on KDM5 subfamily rather than a general effect on all JHDMs (Figure 4A-B). At higher concentrations, H3K27 tri-methylation seems even to decrease, possibly due to regulatory cross-talk effects. To assess whether RS 5033 perturbs cell cycle dynamics as previously observed with RS 3195, we performed a flow cytometry analysis on MCF-7 cells treated with 10 μM and 30 μM of RS 5033. The strong increase of cells in G2/M noted upon treatment with 30 μM of RS 3195 was not observed when MCF-7 cells were treated with RS 5033 (SM Figure S6-7). Moreover, Real Time PCR analysis indicated that RS 5033 treatment induces only a small increase the genes involved in AhR pathway that were found to be upregulated upon RS 3195 treatment, suggesting that RS 5033 stimulates this pathway to a much lesser extent compared to RS 3195 (SM Figure S8). Based on these results, RS 5033 proved to be a selective inhibitor of KDM5 enzymes that does not affect cell cycle nor significantly stimulates AhR response.

**Table 2.** *in vitro* IC<sub>50</sub> of RS 3195, RS 5033 and KDOAM-25 toward KDM5 enzymes

Compound	IC <sub>50</sub>	Reference
RS 3195	2 μM	Mannironi et al., 2014
RS 5033	1 μM	This work
KDOAM-25	<0,1 μM	Tumber et al., 2017

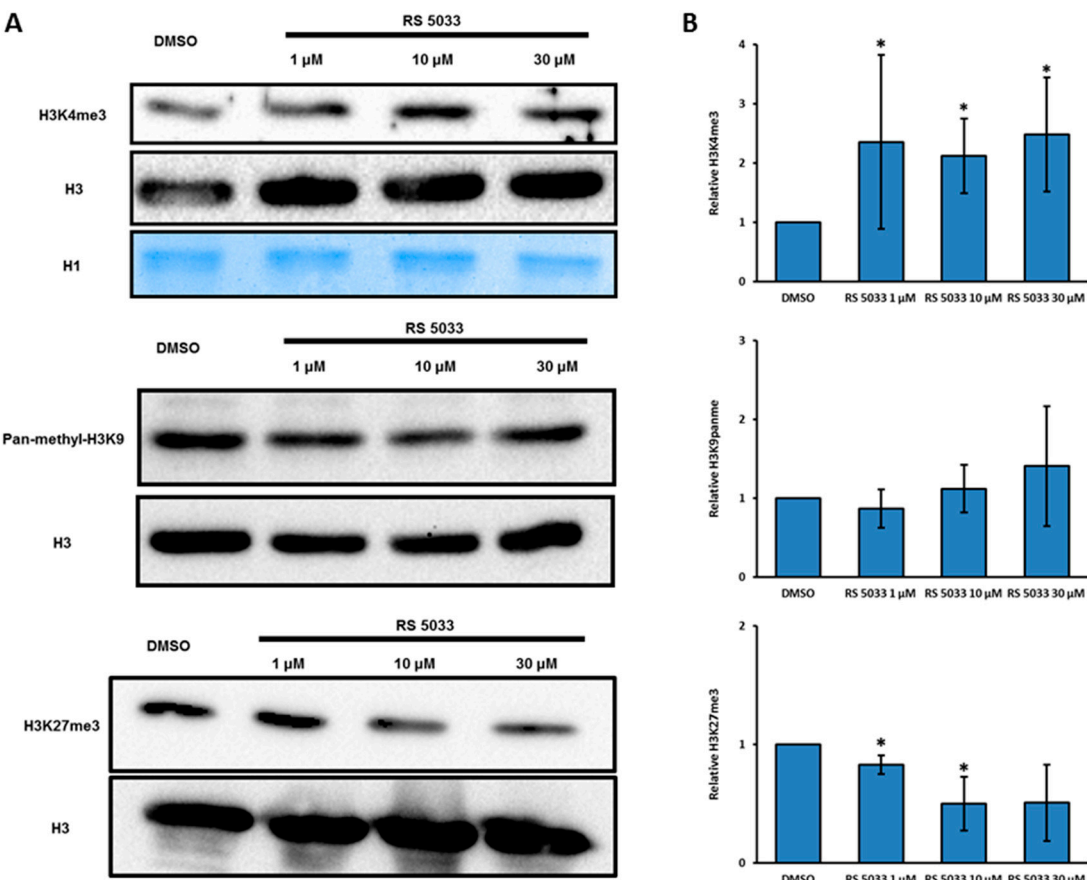


**Figure 4.** RS 5033 is a selective KDM5 enzymes inhibitor. (A) Western blotting analysis of H3K4me3, pan-methyl-H3K9 and H3K27me3 levels in MCF-7 cells after 24 hours of incubation with three different concentrations of RS 5033. Shown images are representative from at least three independent experiments. (B) Quantification of independent western blotting experiments indicating a strong and significant increase of H3K4me3 levels upon treatment with all three concentrations of RS 5033. H3K9me3 levels are not affected whereas H3K27me3 levels decrease upon treatment. Data are normalized to DMSO control and represented the mean ± SD of relative modified histone levels. Statistical significance was assessed according to two-tailed paired Student’s t test. \* p<0.05

We also tested KDOAM-25 [48], a recently characterized potent and specific KDM5 enzymes inhibitor with biochemical half maximal inhibitory concentration values of <100 nM for KDM5A-D *in vitro*. This compound proved to be highly selective toward other 2-OG oxygenases sub-families, and to exert no off-target activity on a panel of 55 receptors and enzymes [48]. KDOAM-25 was reported to inhibit H3K4me3 demethylation of H3K4me3 at transcription start sites and to block proliferation of MM1S multiple myeloma cells [48]. In our hands the compound leads to a modest



(around 1.5-fold) but significant increase of H3K4 tri-methylation in MCF7 bulk chromatin at concentrations 0.03-1  $\mu$ M, while the effect is lost at higher concentrations (Figure 5A-B). As RS 5033 also this compound does not show any significant effect on cell cycle in the same range of concentrations (not shown).

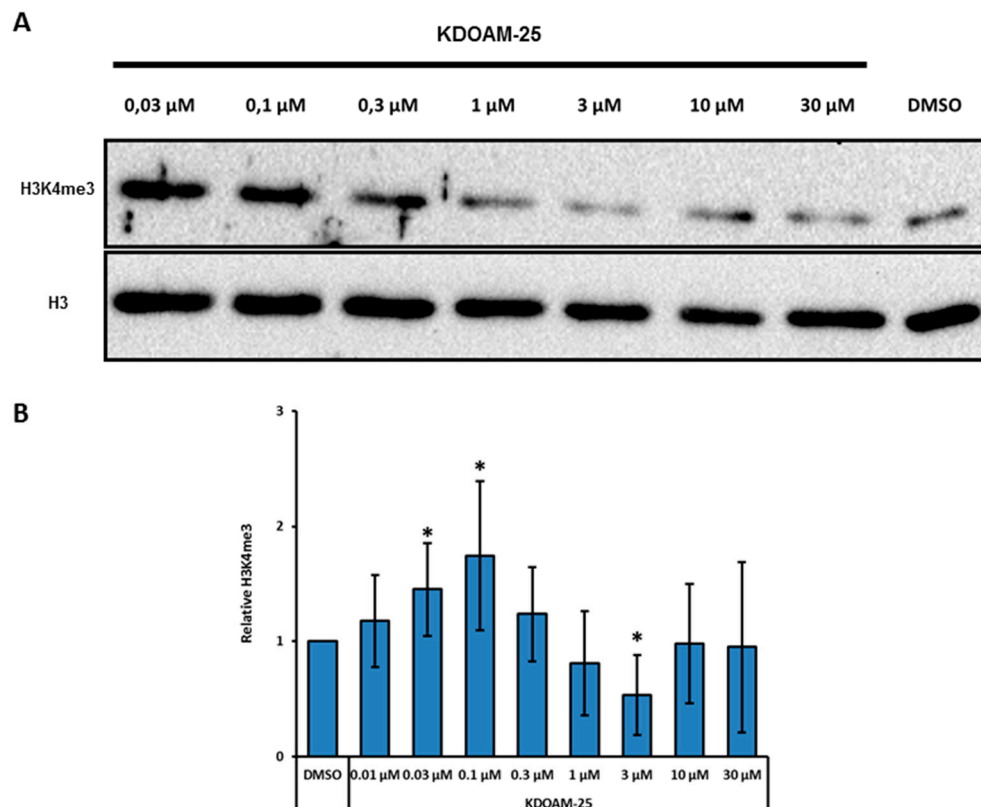


**Figure 5.** KDOAM-25 is a KDM5 enzymes inhibitor that increases H3K4me3 levels at lower concentration in MCF-7 cells. (A) Western blotting analysis of H3K4me3 levels in MCF-7 cells incubated for 24 hours with different concentrations of KDOAM-25. Shown image is representative of four independent experiments. (B) Quantification of independent western blotting experiments, showing a slight increase in H3K4me3 levels upon KDOAM-25 treatment at lower concentration. Data are normalized to DMSO control and represented as the mean  $\pm$  SD of relative H3K4me3 levels. Statistical significance was assessed according to two-tailed paired Student's t test. \*  $p < 0.05$

#### 2.4. KDM5 enzymes inhibition leads to differential expression of selected genes

The best characterized function of KDM5 enzymes is to regulate gene expression. Nevertheless, transcriptome analysis of siKDM5B breast cancer cells indicated that loss of KDM5B does not strongly affect global gene transcription but rather alters transcription of selected genes. Based on available data of transcriptome analysis of siKDM5B in MCF-7 cells [41,49] and of RS 3195 treatment (this work), we selected a set of relevant genes in breast cancer oncogenesis whose regulation could be influenced by inhibition of KDM5 activity and analyzed their expression upon RS 5033 and KDOAM-25 treatment. Among the best-known targets of KDM5B there is BRCA1, a gene well known to play a role in DNA repair and found to be up-regulated upon KDM5B knock down in MCF-7 [17].

Transcriptomic analysis by DNA microarrays, followed by ChIP assays confirmed BRCA1 as a target gene of KDM5B and showed that KDM5B controls also the expression of several members of the metallothionein (MT) family and genes required for a functional G2/M and/or spindle checkpoint. Among the MT genes, MT2A was also found to be downregulated in siKDM5B MCF-7

cells and upon RS 3195 treatment whereas MT1F was reported downregulated by overexpression of KDM5B. Another interesting gene upregulated both by KDM5B silencing and RS 3195 is AKR1C2. This gene is an onco-suppressor as it metabolizes progesterone, producing a catabolite which contributes to suppress cell proliferation in breast cancer [50]. RS 3195 treatment induces also a differential expression of another gene involved in breast cancer, PCDH10, coding for a protocadherin whose transcriptional silencing and promoter methylation were frequently detected in breast carcinoma cell lines [51]. We analyzed the transcript levels of this set of genes on MCF-7 cells treated for 24 hours with RS 5033 and KDOAM-25. At concentrations that proved to induce the strongest increase of H3K4 tri-methylation on MCF-7 cells: 10  $\mu$ M and 30  $\mu$ M for RS 5033 and 0,01  $\mu$ M, 0,03  $\mu$ M and 0,1  $\mu$ M for KDOAM-25. Real Time PCR analysis on RS 5033 treated cells showed no significant modulation of BRCA1 and MT1F genes (SM Figure S9). KDOAM-25, on the other hand, seems to induce a slight increase of the expression of these two genes, even though up-regulation appears to be statistically significant only for BRCA1 at 0,01  $\mu$ M dose with a modest increase (around 1.4-fold). AKR1C2 levels resulted increased by both inhibitors, confirming downregulation of this gene by KDM5B (SM Figure S10). PCDH10 resulted significantly downregulated by 30  $\mu$ M RS 5033 and by 0,01  $\mu$ M and 0,1  $\mu$ M KDOAM-25 (SM Figure S9-10). In table 3 is reported a summary of the results compared to RS 3195 RNA-seq experiment and to literature data. Taken together, our findings seem to confirm the role of KDM5 enzymes as fine-tuners rather than true regulators of the expression of selected oncogenes.

**Table 3.** Summary of transcriptional modulations of genes involved in breast cancer.

Gene	RS 5033 treatment	KDOAM-25 treatment	RS 3195 RNA seq	KDM5 silencing (Yamamoto et al., 2014)	KDM5 silencing (Scibetta et al., 2007)	KDM5 knock down (Yamane et al., 2007)
BRAC1	No modulation	Slight increase	N/A	N/A	N/A	UP
MT1F	No modulation	No modulation	N/A	N/A	UP	N/A
AKR1C2	UP	UP	UP	UP	N/A	N/A
PCDH10	DOWN	DOWN	DOWN	DOWN	N/A	N/A

## 2.5. KDM5 enzymes inhibition increases breast cancer cells sensitivity to ionizing radiation

Besides the well documented role of KDM5 enzymes in transcriptional regulation, recent findings indicate a novel function for KDM5 enzymes in maintaining genome stability. KDM5A and B were reported to play a crucial role in DDR [23-24,52]. To test the hypothesis that inhibiting KDM5 enzymes could impair the ability of the cell to achieve a correct DDR, we irradiated MCF-7 cells with increasing doses of X-ray (0,3 Gy, 1 Gy and 3 Gy) after treatment with three different concentrations of RS 3195 (3  $\mu$ M, 10  $\mu$ M or 30  $\mu$ M); RS 5033 (3  $\mu$ M, 10  $\mu$ M or 30  $\mu$ M) or KDOAM-25 (0,03  $\mu$ M 0,1  $\mu$ M and 0,3  $\mu$ M) in the growth medium. After irradiation cell viability was tested by CCK-8 assay (see Materials and Methods, Figure 6A-C). This analysis showed that when MCF-7 cells are irradiated with 3 Gy there is a significant reduction of viable cells in presence of all the concentrations of RS 5033 and KDOAM-25 compared to DMSO control. RS 3195 shows a more limited effect. To test if this increase of radio-sensitivity produces effects in proliferative activity, we performed a clonogenic assay [53]. This assay allows to evaluate the differences in the capacity of cells to produce progeny between control untreated cells and cells treated with a chemical compound and exposed to X-ray. By calculation of the plating efficiency and survival fractions after exposure of cells to radiation both in untreated and treated cells, it is possible to set out a radiation dose-response curve for X-ray irradiated cells. MCF-7 cells were treated either with DMSO, 10  $\mu$ M RS 5033, 10  $\mu$ M RS 3195 or 0.03

$\mu\text{M}$  KDMOA-25 and then irradiated with 0 Gy, 1 Gy, 3 Gy or 10 Gy (Fig. 6D-F). A slight but significant decrease of proliferative capacity of MCF-7 cells was observed for 3 Gy irradiation dose after RS 5033 and for 3 and 10 Gy after KDMOA-25 treatment compared to DMSO control, while no significant effect was observed for the RS 3195 treatment.

These observations seem to confirm the recently proposed hypothesis that KDM5 enzymes are crucial regulators of genome stability [23-24,52].

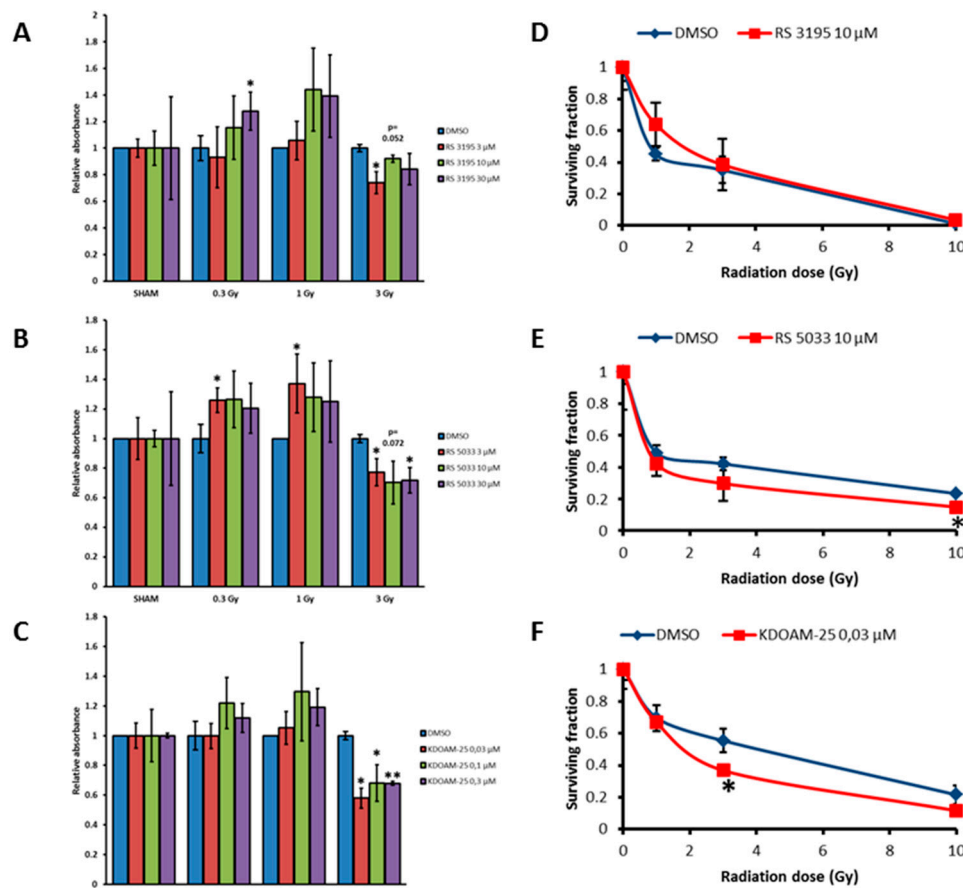


**Figure 6.** KDM5 enzymes inhibition increases breast cancer cells sensitivity to ionizing radiation. (A-C) Viability assay on MCF-7 cells irradiated and treated with three different concentration of RS 3195 (A), RS 5033 (B) or KDOAM-25 (C). The histogram reports the mean of relative absorbance measured at 450 nm  $\pm$  SD from three independent experiments. In order to appreciate the effect of the inhibitors on cell viability in each dose of radiation compared to DMSO control, the absorbance of each dose of radiation (sham, 0.3, 1 and 3 Gy) was normalized to the corresponding DMSO control and then, for each concentration of inhibitors, these values were normalized to the corresponding sham control of alive cells and represent the average. (D-F) Clonogenic assay of MCF-7 cells treated with RS 3195 10  $\mu\text{M}$  (D), RS 5033 10  $\mu\text{M}$  (E) or KDOAM-25 0.03  $\mu\text{M}$  (F) and irradiated with 0 Gy, 2 Gy 5 Gy or 10 Gy X-rays. After the irradiation, cells are seeded again and incubated for 1 day with inhibitor and stained with methylene blue after 13 days. For every dose it is indicated the mean value of the cell survival  $\pm$  SD of 3 independent colony forming assays. Data are normalized to corresponding sham controls. Statistical significance was assessed according to two-tailed paired Student's t test. \*  $p < 0.05$ ; \*\*  $p < 0.001$

## 2.6. Effects of KDM5 inhibitors on H2AX phosphorylation

To test the hypothesis that the observed effects of KDM5 inhibitors in enhancing the radio-sensitivity of the MCF7 cells is due to less efficient DNA damage signaling and repair, we tested the dynamics of H2AX phosphorylation following irradiation in MCF7 cells treated with the

three different compounds. As a consequence of genotoxic damage, phosphorylated H2AX ( $\gamma$ H2AX) accumulates in the nucleus, not exclusively at damaged sites but proportionally to the extent of damage. Its total increase, which can be measured by western blot, is more persistent than its increase at the damaged sites ( $\gamma$ H2AX foci) and can be used to estimate the total amount of damage [54]. Fig.7A shows that irradiation with 6 Gy of X-rays leads to  $\gamma$ H2AX accumulation in MCF7 cells. Treatment with both RS 5033 and KDOAM-25 increases the amount of  $\gamma$ H2AX both in sham-irradiated and in irradiated cells. When normalized to the amount of H2AX (which is also induced by irradiation) the  $\gamma$ H2AX increase is statistically significant at 4h and 24h in RS5033 treated cells while it is not significant in KDOAM-25 treated cells, due to higher variability (Fig. 7B).

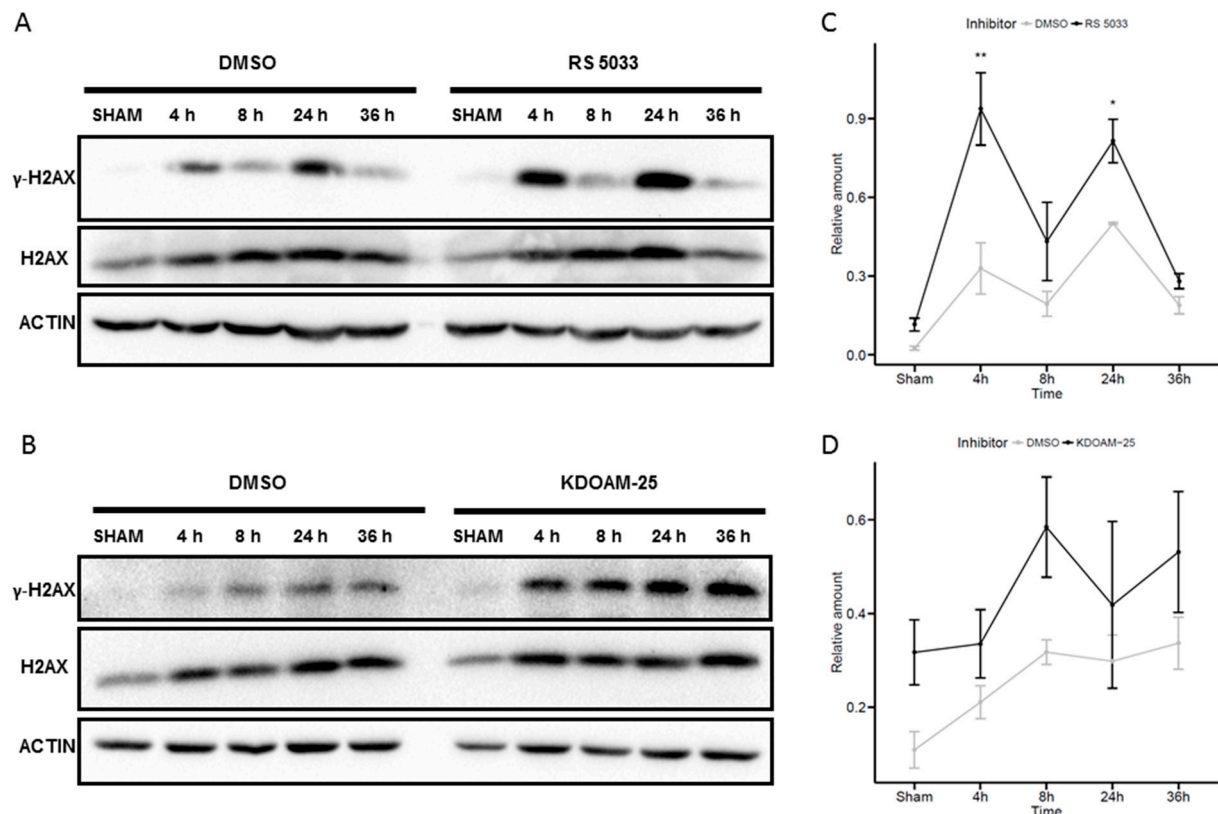


**Figure 7.** KDM5 inhibition increases H2AX phosphorylation. Western blotting analysis of  $\gamma$ -H2AX levels of irradiated MCF7 cells. MCF-7 cells treated with RS 5033 10  $\mu$ M (A) or KDOAM-25 0.03  $\mu$ M (B) are exposed to 0 or 6 Gy of X-rays and irradiated samples are collected after 4, 8, 24 or 36 hours. Shown images are representative from at least two independent experiments. (C-D) Quantification of independent Western blotting experiments, showing an increase in H2AX phosphorylation levels upon RS 5033 and KDOAM-25 treatment. Data are represented as the mean  $\pm$  SD of relative  $\gamma$ H2AX levels (normalized to total H2AX). Statistical significance was assessed according to one-way ANOVA. \* p<0.05; \*\* p<0.001

### 3. Discussion

KDM5 enzymes are histone lysine demethylases acting on H3K4. These enzymes, belonging to the family of JHDMs, are hydroxylases capable of erasing H3K4me2 and H3K4me3 marks. For this reason, KDM5 enzymes were initially proposed to be mainly epigenetic regulators of gene transcription and chromatin organization. However recent findings are suggesting that these enzymes are critical regulators of other important cellular processes, including DNA replication, cell

cycle dynamics and DNA damage repair. Importantly, histone lysine demethylases seem even to catalyze other hydroxylation reactions that regulate both protein and nucleic acid-based processes, or to perform novel functions not relying on their demethylases activity, such as acting as molecular scaffold exploiting their chromatin-binding capacity to recruit other proteins and chromatin remodeling activities [55].

In view of all this, developing small molecules capable of inhibiting this subfamily of JHDMs and finding novel mechanisms of regulation of their expression could be helpful to investigate their emerging functions. Since there are growing evidences linking KDM5 enzymes deregulation to several types of tumors, acting on them by epigenetic inhibitors could shed light on the role of these proteins in cancer onset and pave the way to new strategies of therapy. In particular, KDM5A (JARID1A/RBP2) and KDM5B (JARID1B/PLU1) contribute to cancer cell proliferation, reduce the expression of tumor suppressor genes, promote the development of drug tolerance and maintain tumor initiating cells.

In this work we tried to define a role for KDM5 enzymes in breast cancer cells, a cellular context in which the major role of these histone demethylases is well established. First, we found a compound, named RS 5033, capable of specifically inhibiting the catalytic mechanism of KDM5 enzymes. This molecule derives from a previous compound (RS 3195) identified a screening in *Saccharomyces cerevisiae* of 45 compounds predicted to mimic the  $\alpha$ -ketoglutarate cofactor of the enzymes [36]. Although RS 3195 seemed to consistently increase H3K4me3 levels both in yeast and in HeLa cells, it appears less effective in breast cancer cell line MCF-7 overexpressing KDM5B. Nevertheless, we analyze its effects on MCF-7 transcriptome. The most remarkable modulation caused by RS 3195 in the gene expression profile of MCF-7 cells was the up-regulation of the genes involved in aryl-hydrocarbon response, a pathway involved in the regulation of biological responses to planar aromatic (aryl) hydrocarbons, suggesting a potential toxic effect of our compound. Thus, we moved on RS 5033 that proved to be more effective in binding the catalytic site of KDM5 enzymes and not to stimulate the AhR pathway. In a range of concentrations between 1 and 30  $\mu$ M, RS 5033 significantly increases tri-methylation of H3K4 in MCF-7 without increasing methylation of other lysines whose demethylation is not under direct control of KDM5 enzymes. Indeed, H3K27 tri-methylation seems even to decrease at highest concentration of inhibitor (about two-fold) through a still elusive mechanism. One speculation is the possibility of a cross-talk between these two histone modifications by which an increasing of H3K4me3, which has a positive effect on gene transcription, could indirectly lower the levels of H3K27me3, which on the contrary is correlated with gene repression. We analyzed also the effect on bulk chromatin of KDOAM-25, a new compound that proved to inhibit KDM5 enzymes *in vitro* with a  $IC_{50}$  <100 nM. In MCF-7 cells, this molecule induces a slight increase of H3K4me3 levels at lower concentrations (0.03-1  $\mu$ M) whereas no effect is observed at higher doses. We used RS 3195, RS 5033 and KDOAM-25 inhibitors to investigate the role of KDM5 enzymes in transcriptional regulation in breast cancer cells. Based on our transcriptome data using RS 3195 and on data on KDM5B silencing available in literature, we found some genes potentially regulated by KDM5 enzymes. Among these, *AKR1C2* is noteworthy because it catabolizes progesterone in 3  $\alpha$  HP that suppresses cell growth [50]. In accordance with data from KDM5B silencing experiment, *AKR1C2* was found to be upregulated upon RS 3195, RS 5033 and KDOAM-25 treatment. This result corroborates the involvement of KDM5 enzymes in the regulation of this gene, suggesting a potential mechanism linking KDM5B to cell growth deregulation in breast carcinoma. *PCDH10*, a gene coding for a protocadherin, also resulted to be downregulated upon treatment with all three inhibitors. Once again, this outcome correlates with data of Yamamoto and colleagues. Strikingly, the expression of two of the first characterized KDM5B targets, *BRCA1* and *MT1F*, resulted essentially unaffected by KDM5 inhibition. These findings indicate, as previously reported, that KDM5 enzymes do not regulate gene expression at a global scale but rather modulate transcript levels at specific genomic regions and in a context-dependent way.

Next, we used these inhibitors to investigate the emerging function of KDM5 enzymes in genome stability maintenance. Thus, we tested their effects on MCF7 cells radio-sensitivity. All three



molecules led to a decrease in short-term viability of irradiated MCF-7 cells. As regard long-term effects of radiation, RS 5033 and KDOAM-25 treatment decreased the capacity of forming clones in MCF-7 cells exposed to X-ray, whereas such effect appeared not evident in the case of RS 3195. We also tested the effects of RS 5033 and KDOAM-25 treatment on the kinetics of accumulation of  $\gamma$ -H2AX, which has been shown to correlate with DNA damage. Treatment with both compounds leads to an evident increase of  $\gamma$ -H2AX accumulation in sham-irradiated cells and between 4 and 24 hours after irradiation as compared with untreated cells. Taken together, these experimental evidences revealed that chemical inhibitors targeting KDM5 enzymes increases sensitivity to spontaneous and X-ray-induced damage. Our results are in line with recent discoveries emphasizing the relevance of histone demethylase as key players of genome stability. According to a recent study, the chemical inhibition of another histone lysine demethylase, KDM6A (UTX), results in enhanced radio-sensitivity of three different tumor cell lines, including MDA-MB-231 triple-negative breast tumor cells [56]. In view of this, a future therapy relying on inhibition of histone lysine demethylases by small molecules to sensitize tumor cells to irradiation appears particularly promising.

## 4. Materials and Methods

### 4.1. Cell cultures

MCF-7 human breast cancer cells were purchased from ATCC (ATCC-LGC Standards). Cells were grown in adherence in high glucose Dulbecco's Modified Eagle Medium (DMEM) (#FA30WL0101500, Carlo Erba) with 1% penicillin/streptomycin (#P11-010, PAA), 2 mM L-Glutamine (#M11-004, PAA), 10% previously inactivated Fetal Bovine Serum (#A15-101, PAA). Cells were maintained at 37°C and 5% CO<sub>2</sub> in an incubator (Thermo Forma Series II Water Jacketed CO<sub>2</sub> Incubator) and routinely passaged removing DMEM, washing with PBS (#FA30WL0615500, Carlo Erba) and detaching them using a suitable amount of Trypsin/EDTA (#T4299-100ML, Sigma-Aldrich).

### 4.2. RNA-sequencing

Total RNA was extracted and quantified as previously described. RNA-Seq libraries preparation and sequencing was performed by the IGA Technology Services (Udine, Italy) using the Illumina TruSeq RNA Sample Preparation Kit V2 (Illumina, San Diego, USA) according to manufacturer's instructions. The final libraries for single-read sequencing of 50 base pairs were carried out on an Illumina HiSeq2000. Each sample produced about 20 million of reads. Reads quality was evaluated using FastQC (version 0.11.2, Babraham Institute Cambridge, UK) tool, then reads were mapped to the mouse Ensembl GRCm38 build reference genome using Tophat (version 2.0.12) [57] with the default settings added with the “—no-novel-juncs” option. Gene structure annotations corresponding to the Ensembl annotation release 75 were used to build a transcriptome index and provided to Tophat during the alignment step using the “-G” parameter. The same gene annotation was used to quantify the gene-level read counts using HTSeq-count (version 0.6.1) script, subsequently the differential analyses for gene expression were performed using Bioconductor [58] R (version 3.2.2) (R Core Team, 2015) package DESeq2 (version 1.4.5). The resulting filtered (adjusted p-value < 0.1) genes were clustered by enrichment pathway analysis using Bioconductor R packages ClusterProfiler [59] and with Gene Ontology Database [60].

### 4.3. Surface Plasmon Resonance (SPR)

Surface Plasmon Resonance (SPR) experiments were carried out using a SensiQ Pioneer system. Immobilization of ligand (KDM5D) was carried out essentially as in Ilari et al. [61]. The sensor chip (COOH5) was activated chemically by a 100  $\mu$ l injection of a 1:1 mixture of

N-ethyl-N'-(3-(diethylaminopropyl)carbodiimide (200 mM) and N-hydroxysuccinimide (50 mM) at a flow rate of 5  $\mu$ l/min. KDM5D was immobilized on activated sensor chips via amine coupling. The immobilization was carried out in 20 mM sodium acetate at pH 4.5; the remaining unreacted groups were blocked by injecting 1 M ethanolamine hydrochloride (100  $\mu$ l). The amount of immobilized KDM5D was detected by mass concentration-dependent changes in the refractive index on the sensorchip surface and corresponded to about 11000 resonance units (RU); an empty flow cell was used as a reference. Analytes, i.e. inhibitors RS3152, RS3183, RS3195, RS4995 and RS5033 were dissolved in DMSO at a concentration of 10 mM and diluted in HSP buffer (10 mM Hepes pH 7.4, 150 mM NaCl + 0.005% surfactant P20) to yield 100  $\mu$ M inhibitor concentration in HSP + 1% DMSO (HSP-1%D). The analytes were automatically diluted in HSP-1%D and injected on the sensorchip for 120 s at a constant flow (30  $\mu$ l/min); analyte concentrations were: 1) 6.25  $\mu$ M; 2) 12.5  $\mu$ M; 3) 25  $\mu$ M; 4) 50  $\mu$ M; 5) 100  $\mu$ M. The increase in RU relative to baseline indicates complex formation; the plateau region represents the steady-state phase of the interaction, whereas the decrease in RU after 120 s represents dissociation of analytes from immobilized KDM5 after injection of buffer HSP-1%D. The sensorgrams were analysed using the SensiQ Qdat 4.0 program and using simple Scatchard plots.

#### 4.4. Chemical compounds

##### Molecular Modelling

All molecular modelling studies were performed on a MacPro dual 2.66 GHz Xeon running Ubuntu 16LTS. The KDM5B structures were downloaded from PDB [<http://www.rcsb.org/>] Pdb code: 5FPL. [46-47]. Hydrogen atoms were added to the protein using Maestro (Small-Molecule Drug Discovery Suite 2015-1, Schrödinger, LLC, New York, NY, 2017) protein preparation wizard [62]. Ligand structures were built with Maestro and minimized using the MMFF94x force field until a rmsd gradient of 0.05 kcal/mol/ $\text{\AA}^2$  was reached. The docking simulations were carried out by Plants [63]. The images depicted in the manuscript were generated by Pymol (PyMOL version 1.2r1; DeLanoScientificLLC: SanCarlos, CA <http://www.pymol.org/>). The residues are numbered according to the crystal structure sequence.

KDOAM-25 was purchased from Sigma-Aldrich (#SML1588).

#### 4.5. Enzymatic inhibition assay

Inhibition by RS5033 (IC<sub>50</sub>) was determined by The *Epigenase*<sup>TM</sup> JARID Demethylase Activity/Inhibition Assay Kit (Fluorometric) (#P-3083-48 Epigentek) which is a complete set of optimized reagents, designed for an easy and fast fluorometric measurement of JARID activity or inhibition. The antibody-based, immune-specific method directly detects JARID-converted demethylated products, rather than by- products, in a 96 stripwell microplate format.

#### 4.6. Protein analysis

##### 4.6.1. Protein isolation

Total protein isolation was performed with RIPA buffer. DMEM was removed, cells were washed with Dulbecco's Phosphate Buffered Saline (PBS, #FA30WL0615500, Carlo Erba Reagents) and then resuspended in 80  $\mu$ l RIPA buffer (#R0278-50ML Sigma-Aldrich) with phosphatase inhibitor (Phosphatase Inhibitor Cocktail 2, #P5726, and Phosphatase Inhibitor Cocktail 3, #P0044, Sigma-Aldrich) and protease inhibitor cocktail (Complete Tablets, Mini EDTA-free, #04693159001, Roche, Mannheim, Germany). Proteins were extracted according to producer's protocol guidelines and stored at -20°C until use. BIORAD Quick Start Bradford Dye assay (#5000205) was used to assess protein concentration.

Histone isolation was performed according to acid extraction of histones protocol of Shechter and colleagues [64]. Histone concentration was determined by running 5  $\mu$ l of samples and known

concentrations of commercially available purified calf thymus histones (from Sigma Aldrich Cat. #000000010223565001) on a SDS-PAGE gel. The gel is stained with Coomassie blue G 250 (BIO-RAD Cat. #161-0786) for 1 hour at room temperature and then destained in distilled water. The gel image is acquired with ChemiDoc XRS+ Imaging System (Bio-Rad) and the volumes of bands of the samples are compared to standard concentrations of calf thymus histone.

#### 4.6.2. Western blotting analysis

Proteins were resolved on a 12% denaturing polyacrylamide gel, using either 4 µg of histone preparation or 40 µg of cell lysate. After electrophoresis, proteins were transferred on a nitrocellulose membrane (Amersham™ Protran™ 0.45 µM NC, # 10600002) via wet transfer method using a Bio-Rad tank. Transfer efficiency was verified via ponceau staining (#P7767, Sigma Diagnostics). Filters were blocked with either milk (#70166, Sigma-Aldrich) or Bovin serum albumin (#A3069, Sigma-Aldrich) and then hybridized over night at 4 °C in gentle rotation with the following antibodies: rabbit anti-H3K4me3 (1:1000, #39915, Active Motif, RRID:AB\_2687512); rabbit-anti-H3K27me3 (1:1000, #9733, Cell Signaling Technology, RRID:AB\_2616029); rabbit-anti-H3K9pan-methylated (1:1000, #4473, RRID:AB\_10544693); rabbit-anti-H3 (1:100000, Cat#1791, ABCAM, RRID:AB\_302613); rabbit anti-H2AX (1:1000, Cat#7631, Cell Signaling Technology, RRID:AB\_10860771), rabbit anti-Phospho-H2AX (1:1000, Cat#9718, Cell Signaling Technology, RRID:AB\_2118009). Goat-anti-Rabbit Horseradish Peroxidase conjugated (1:10000, #31460, Thermo Fisher Scientific, RRID:AB\_228341) was used as secondary antibody for 1 hour hybridization at room temperature. Blots were scanned and analyzed with a ChemiDoc XRS+ Imaging System (Bio-Rad). The volumes of each band of protein was acquired using Bio-Rad's ImageLab software by means of volume tools using global quantification. The signal for each protein was normalized to the housekeeping protein and ratios with average control values were determined.

For histones as loading control was used either total histone H3 detected by a specific antibody or histone H1 levels by staining the upper part of the gel properly cut before protein transfer on nitrocellulose membrane.

#### 4.7. Gene expression analysis

##### 4.7.1. RNA extraction and reverse transcription

Total RNA from treated cells was isolated using miRNeasy® mini kit (#217004, Qiagen), according to producer's protocol guidelines. One µg of total RNA was reverse-transcribed using QuantiTect® Reverse Transcription Kit (#205311, Qiagen), according to producer's protocol guidelines (Qiagen).

##### 4.7.2. Quantitative RT-PCR

Relative quantification of gene expression was performed with the Applied Biosystems 7500 Real Time PCR System using SensiFAST™ SYBR® Lo-ROX Kit (#BIO 94020, Bioline). The relative amount of mRNA expression was determined by means of  $\Delta\Delta C_t$  method [65], using GAPDH as internal control. Primers were designed using [www.ncbi.nlm.nih.gov/tools/primer-blast/](http://www.ncbi.nlm.nih.gov/tools/primer-blast/) and purchased from Sigma-Aldrich. The following oligos were used:

BRCA1 mRNA:

- Fw: 5'- GGAGTGGAAAGGTCATCCCC -3'

BRCA1 mRNA:

- Rv: 5'- TGAGCTCCTCTTGAGATGGGT -3'

MT1F mRNA:

- Fw: 5' - TCCTGCAAGTGCAAAGAGTG-3'

MT1F mRNA:

- Rv: 5' - AAAGGTTGTCCTGGCATCAG-3'  
 CYP1A1 mRNA:  
 - Fw: 5'- CCCACAGCACAACAAGAGA-3'  
 CYP1A1 mRNA:  
 - Rv: 5'- CAGGGGTGAGAAACCGTTCA-3'  
 AHRR mRNA:  
 - Fw: 5'- CAATTACTCAGCAGGAAGGAGC-3'  
 AHRR mRNA:  
 - Rv: 5'- CTTGGGGTCAAGGACAAGGTC-3'  
 AKR1C2 mRNA:  
 - Fw: 5'- CCAGTGTCTGTAAAGGAGGACA-3'  
 AKR1C2 mRNA:  
 - Rv: 5'- ACATGCAATCACGGAAGTATGG-3'  
 PCDH10 mRNA:  
 - Fw: 5'- GTGCAAACGTGTTCGCAGAT-3'  
 PCDH10 mRNA:  
 - Rv: 5'- TTTCTGCCAATCCTGGGGTTC-3'  
 GAPDH mRNA:  
 - Fw: 5'- TCCTCTGACTTCAACAGCGAC-3'  
 GAPDH mRNA:  
 - Rv: 5'- CGTTGTCATACCAGGAAAT-3'

#### 4.8. Clonogenic assay

One hour after treatment with inhibitors, cells were exposed to X-ray using a Gilardoni MLG 300/6-D apparatus set to 200 V and 6 mA, in order to produce an equivalent absorbed dose of 1cGy/s. Afterwards, cells were harvested, counted and then diluted in inhibitor containing growth medium. Appropriate cell numbers were seeded in quadruplicate according to the doubling time of the cell line and to radiation dose. 24 hours after this seeding, the medium with inhibitor was replaced with fresh DMEM and cells were then incubated for 14 days (enough time to allow at least six cell divisions). After this period of growth, cells were washed twice with PBS and then fixed and stained with a suitable volume of a solution made of 0.3% Methylene Blue and 80% Ethanol for 30 minutes at room temperature. After washing cells twice with ddH<sub>2</sub>O, plates were pictured with ChemiDoc XRS+ Imaging System (Bio-Rad) in colorimetric mode. Colonies were detected using Fiji software [66], with the "Find maxima" function setting a background noise threshold of 3000. Radiation-dose response curves to X-ray for DMSO and inhibitor samples were calculated using surviving fraction. Plating efficiency and surviving fraction were calculated as follows:

Plating efficiency = number of colonies counted / number of cells plated

Surviving fraction = Plating efficiency / plating efficiency of shame sample

#### 4.9. Cytotoxicity assay

The cytotoxicity assay was performed with Cell Counting Kit-8 (#96992, Sigma-Aldrich) according to the manufacturer's instructions. 100 µl of MCF-7 cell suspension (5000 cells/ well) was dispensed in a 96-well plate. After 24 hours, inhibitor or DMSO was added in growth medium and then cells were irradiated. 48 hours post irradiation, 10 µl of CCK-8 solution was added to each well of the plate and incubated again for 1 hour. Incubate the plate for 1-4 hours in the incubator. The absorbance at 450 nm was read using a Wallac VICTOR2 1420. The absorbance at 450 nm of each sample, which is proportional to the number of viable cells, was first normalized on the same value of absorbance of blank (a well with only growth medium). The absorbance of each dose of radiation

(sham, 0.3, 1 and 3 Gy) was normalized to the corresponding DMSO control and then, for each concentration of inhibitors, these values were normalized to the corresponding sham control.

#### 4.10. Flow-cytometry

Flow-cytometry analysis of DNA content was carried out using an EPICS xl flow-cytometer (Beckman-Coulter). DMSO and inhibitor treated MCF-7 cells were trypsinized, pelleted, washed with PBS and finally resuspended in PBS containing 0.1% Triton-X-100 (#A1388.1000, AppliChem) and 40 µg/ml propidium iodide (#P-4170, Sigma). After 20 min incubation at 37 °C the samples were analyzed. 10000 events were acquired for each sample. Acquired data were analyzed using the WinMDI software by Joe Trotter, available at <http://facs.scripps.edu>

**Acknowledgments:** This work has been supported by Sapienza University grant: RM11715C53A3F678. We thank Dr. Roberto Contestabile for help in setting up the assay for HDMs inhibitors.

**Author Contributions:** S.P., R.S., A.C., V.L., A.M. and R.N. conceived and designed the experiments; S.P., C.M., V.L., L.B., G.C., E.C., V.N. and G.L.R., performed the experiments; S.M., C.M., G.C., E.C. and V.L. analyzed the data; A.M. and G.L.R. contributed reagents/materials/analysis tools; S.P., R.S. and R.N. wrote the paper.

**Conflicts of Interest:** The authors declare no conflict of interest

#### Abbreviations

The following abbreviations are used in this manuscript:

KDM: histone lysine demethylase

LSD: Lysine Specific histone Demethylase

JHDMS: Jumonji Histone Demethylases

SPR: Surface Plasmon Resonance

QRT-PCR: Quantitative Reverse Transcription-PCR

IC<sub>50</sub>: half maximal inhibitory concentration

#### References

- Black, J. C.; Van Rechem, C.; Whetstone, J. R. Histone Lysine Methylation Dynamics: Establishment, Regulation, and Biological Impact. *Mol. Cell.* **2012**, *48*(4), 491-507. <https://doi.org/10.1016/j.molcel.2012.11.006> <https://www.ncbi.nlm.nih.gov/pubmed/23200123>
- Martin, C.; Zhang, Y. The diverse functions of histone lysine methylation. *Nat. Rev. Mol. Cell Biol.* **2005**, *6*, 838–849. <http://dx.doi.org/10.1038/nrm1761> <https://www.ncbi.nlm.nih.gov/pubmed/16261189>
- Kouzarides, T. Chromatin Modifications and Their Function. *Cell* **2007**, *128*(4), 693-705. <http://dx.doi.org/10.1016/j.cell.2007.02.005> <https://www.ncbi.nlm.nih.gov/pubmed/17320507>
- Forneris, E.; Binda, C.; Vanoni, M.A.; Mattevi, A.; Battaglioli, E. Histone demethylation catalysed by LSD1 is a flavin-dependent oxidative process. *FEBS Lett.* **2005**, *579*, 2203–2207. <http://dx.doi.org/10.1016/j.febslet.2005.03.015> <https://www.ncbi.nlm.nih.gov/pubmed/15811342>
- Karytinos, A.; Forneris, F.; Profumo, A.; Clossani, G.; Battaglioli, E.; Binda, C.; Mattevi, A. A novel mammalian flavin-dependent histone demethylase. *J. Biol. Chem.* **2009**, *284*, 17775–17782. <http://dx.doi.org/10.1074/jbc.M109.003087> <https://www.ncbi.nlm.nih.gov/pubmed/19407342>
- Klose, J.R.; Kallin, E.M.; Khang, Y. JmJC-domain-containing proteins and histone demethylation. *Nat. Rev. Gen.* **2006**, *7*, 715–727. <http://dx.doi.org/10.1038/nrg1945> <https://www.ncbi.nlm.nih.gov/pubmed/16983801>
- Lohse, B.; Kristensen, J.L.; Kristensen, L.H.; Agger, K.; Helin, K.; Gajhede, M.; Clausen, R.P. Inhibitors of histone demethylases. *Bioorg. Med. Chem.* **2011**, *19*, 3625–3636. <http://dx.doi.org/10.1016/j.bmc.2011.01.046> <https://www.ncbi.nlm.nih.gov/pubmed/21596573>
- Eissenberg, J.C.; Shilatfard, A. Histone H3 Lysine 4 (H3K4) Methylation in Development and Differentiation. *Dev Biol.* **2010**, *339*(2), 240–249. <http://dx.doi.org/10.1016/j.ydbio.2009.08.017> <https://www.ncbi.nlm.nih.gov/pubmed/19703438>



9. Lauberth, S.M.; Nakayama, T.; Wu, X.; Ferris, A.L.; Tang, Z.; Hughes, S.H.; Roeder, R.G. H3K4me3 interactions with TAF3 regulate preinitiation complex assembly and selective gene activation. *Cell* **2013**, *152*, 1021–1036. <http://dx.doi.org/10.1016/j.cell.2013.01.052> <https://www.ncbi.nlm.nih.gov/pubmed/2345285>
10. Santos-Rosa, H.; Schneider, R.; Bannister, A.J.; Sherriff, J.; Bernstein, B.E.; Emre, N.C.; Schreiber, S.L.; Mellor, J.; Kouzarides, T. Active genes are tri-methylated at K4 of histone H3. *Nature* **2002**, *419*, 407–411. <http://dx.doi.org/10.1038/nature01080> <https://www.ncbi.nlm.nih.gov/pubmed/12353038>
11. Outchkourov, N.S.; Muiño, J.M.; Kaufmann, K.; van Ijcken, W.F.; Groot Koerkamp, M.J.; van Leenen, D.; de Graaf, P.; Holstege, F.C.; Grosveld, F.G.; Timmers, H.T. Balancing of histone H3K4 methylation states by the Kdm5c/SMCX histone demethylase modulates promoter and enhancer function. *Cell. Rep.* **2013**, *3*(4), 1071–9. <http://dx.doi.org/10.1016/j.celrep.2013.02.030> <https://www.ncbi.nlm.nih.gov/pubmed/2354550>
12. Blair, L.P.; Cao, J.; Zou, M.R.; Sayegh, J.; Yan, Q. Epigenetic Regulation by Lysine Demethylase 5 (KDM5) Enzymes in Cancer. *Cancers* **2011**, *3*(1), 1383–1404. <http://dx.doi.org/10.3390/cancers3011383> <https://www.ncbi.nlm.nih.gov/pubmed/21544224>
13. Hayami, S.; Yoshimatsu, M.; Veerakumarasivam, A.; Unoki, M.; Iwai, Y.; Tsunoda, T.; Field, H.I.; Kelly, J.D.; Neal, D.E.; Yamaue, H.; Ponder, B.A.; Nakamura, Y.; Hamamoto, R. Overexpression of the JmJc histone demethylase KDM5B in human carcinogenesis: involvement in the proliferation of cancer cells through the E2F/RB pathway. *Mol. Cancer* **2010**, *9*, 59. <http://dx.doi.org/10.1186/1476-4598-9-59> <https://www.ncbi.nlm.nih.gov/pubmed/20226085>
14. Lu, P.J.; Sundquist, K.; Baeckstrom, D.; Poulsom, R.; Hanby, A.; Meier-Ewert, S.; Jones, T.; Mitchell, M.; Pitha-Rowe, P.; Freemont, P.; Taylor-Papadimitriou, J. A novel gene (PLU-1) containing highly conserved putative DNA/chromatin binding motifs is specifically up-regulated in breast cancer. *J. Biol. Chem.* **1999**, *274*, 15633–15645. <http://dx.doi.org/10.1074/jbc.274.22.15633> <https://www.ncbi.nlm.nih.gov/pubmed/10336460>
15. Xiang, Y.; Zhu, Z.; Han, G.; Ye, X.; Xu, B.; Peng, Z.; Ma, Y.; Yu, Y.; Lin, H.; Chen, A.P.; Chen, C.D. JARID1B is a histone H3 lysine 4 demethylase up-regulated in prostate cancer. *Proc. Natl. Acad. Sci. USA* **2007**, *104*, 19226–19231. <http://dx.doi.org/10.1073/pnas.0700735104> <https://www.ncbi.nlm.nih.gov/pubmed/18048344>
16. Zeng, J.; Ge, Z.; Wang, L.; Li, Q.; Wang, N.; Bjorkholm, M.; Jia, J.; Xu, D. The histone demethylase RBP2 is overexpressed in gastric cancer and its inhibition triggers senescence of cancer cells. *Gastroenterology* **2010**, *138*, 981–992. <http://dx.doi.org/10.1053/j.gastro.2009.10.004> <https://www.ncbi.nlm.nih.gov/pubmed/19850045>
17. Yamane, K.; Tateishi, K.; Klose, R.J.; Fang, J.; Fabrizio, L.A.; Erdjument-Bromage, H.; Taylor-Papadimitriou, J.; Tempst, P.; Zhang, Y. PLU-1 is an H3K4 demethylase involved in transcriptional repression and breast cancer cell proliferation. *Mol. Cell.* **2007**, *25*(6):801–12. <http://dx.doi.org/10.1016/j.molcel.2007.03.001> <https://www.ncbi.nlm.nih.gov/pubmed/17363312>
18. Defeo-Jones, D.; Huang, P.S.; Jones, R.E.; Haskell, K.M.; Vuocolo, G.A.; Hanobik, M.G.; Huber, H.E.; Oliff, A. Cloning of cDNAs for cellular proteins that bind to the retinoblastoma gene product. *Nature* **1991**, *352*, 251–4. <http://dx.doi.org/10.1038/352251a0> <https://www.ncbi.nlm.nih.gov/pubmed/1857421>
19. Benevolenskaya, E.V.; Murray, H.; Branton, P.; Young, R.A.; Kaelin, W.G. Jr. Binding of pRB to the PHD protein RBP2 promotes cellular differentiation. *Mol. Cell.* **2005**, *18*, 623–35. <https://doi.org/10.1016/j.molcel.2005.05.012> <https://www.ncbi.nlm.nih.gov/pubmed/15949438>
20. Hidalgo, A.; Baudis, M.; Petersen, I.; Arreola, H.; Piña, P.; Vázquez-Ortiz, G.; Hernández, D.; González, J.; Lazos, M.; López, R.; Pérez, C.; García, J.; Vázquez, K.; Alatorre, B.; Salcedo, M. Microarray comparative genomic hybridization detection of chromosomal imbalances in uterine cervix carcinoma. *BMC Cancer* **2005**, *5*, 77. <http://dx.doi.org/10.1186/1471-2407-5-77> <https://www.ncbi.nlm.nih.gov/pubmed/16004614>
21. Wang, Q.; Wei, J.; Su, P.; Gao, P. Histone demethylase JARID1C promotes breast cancer metastasis cells via down regulating BRMS1 expression. *Biochem. Biophys. Res. Commun.* **2015**, *464*(2), 659–66. <http://dx.doi.org/10.1016/j.bbrc.2015.07.049> <https://www.ncbi.nlm.nih.gov/pubmed/26182878>
22. Klein, B.J.; Piao, L.; Xi, Y.; Rincon-Arano, H.; Rothbart, S.B.; Peng, D.; Wen, H.; Larson, C.; Zhang, X.; Zheng, X.; Cortazar, M.A.; Peña, P.V.; Mangan, A.; Bentley, D.L.; Strahl, B.D.; Groudine, M.; Li, W.; Shi, X.; Kutateladze, T.G. The histone-H3K4-specific demethylase KDM5B binds to its substrate and product through distinct PHD fingers. *Cell Rep.* **2014**, *6*(2), 325–35. <http://dx.doi.org/10.1016/j.celrep.2013.12.021> <https://www.ncbi.nlm.nih.gov/pubmed/24412361>

23. Li, X.; Liu, L.; Yang, S.; Song, N.; Zhou, X.; Gao, J.; Yu, N.; Shan, L.; Wang, Q.; Liang, J.; Xuan, C.; Wang, Y.; Shang, Y.; Shi, L. Histone demethylase KDM5B is a key regulator of genome stability. *Proc. Natl. Acad. Sci. USA* **2014**, *111*(19), 7096-101. <http://dx.doi.org/10.1073/pnas.1324036111> <https://www.ncbi.nlm.nih.gov/pubmed/24778210>
24. Gong, F.; Clouaire, T.; Aguirrebengoa, M.; Legube, G.; Miller, K.M. Histone demethylase KDM5A regulates the ZMYND8-NuRD chromatin remodeler to promote DNA repair. *J. Cell. Biol.* **2017**, *216*(7), 1959-1974. <http://dx.doi.org/10.1083/jcb.201611135> <https://www.ncbi.nlm.nih.gov/pubmed/28572115>
25. Heerboth, S.; Lapinska, K.; Snyder, N.; Leary, M.; Rollinson, S.; Sarkar, S. Use of Epigenetic Drugs in Disease: An Overview. *Genet. Epigenet.* **2014**, *6*, 9-19. <http://dx.doi.org/10.4137/GEG.S12270> <https://www.ncbi.nlm.nih.gov/pubmed/25512710>
26. Højfeldt, J.W.; Agger, K.; Helin, K. Histone lysine demethylases as targets for anticancer therapy. *Nat. Rev. Drug Discov.* **2014**, *12*(12), 917-30. <http://dx.doi.org/10.1038/nrd4154> <https://www.ncbi.nlm.nih.gov/pubmed/24232376>
27. McGrath, J.; Trojer, P. Targeting histone lysine methylation in cancer. *Pharmacol. Ther.* **2015**, *50*, 1-22. <http://dx.doi.org/10.1016/j.pharmthera.2015.01.002> <https://www.ncbi.nlm.nih.gov/pubmed/25578037>
28. Wang, L.; Chang, J.; Varghese, D.; Dellinger, M.; Kumar, S.; Best, A.M.; Ruiz, J.; Bruick, R.; Peña-Llopis, S.; Xu, J.; Babinski, D.J.; Frantz, D.E.; Brekken, R.A.; Quinn, A.M.; Simeonov, A.; Easmon, J.; Martinez, E.D. A small molecule modulates Jumonji histone demethylase activity and selectively inhibits cancer growth. *Nat. Commun.* **2013**, *4*, 2035. <http://dx.doi.org/10.1038/ncomms3035> <https://www.ncbi.nlm.nih.gov/pubmed/23792809>
29. Spannhoff, A.; Hauser, A.T.; Heinke, R.; Sippl, W.; Jung, M. The emerging therapeutic potential of histone methyltransferase and demethylase inhibitors. *Chem. Med. Chem.* **2009**, *4*(10), 1568-82. <http://dx.doi.org/10.1002/cmdc.200900301> <https://www.ncbi.nlm.nih.gov/pubmed/19739196>
30. Hatch, S.B.; Yapp, C.; Montenegro, R.C.; Savitsky, P.; Gamble, V.; Tumber, A.; Ruda, G.F.; Bavetsias, V.; Fedorov, O.; Atrash, B.; Raynaud, F.; Lanigan, R.; Carmichael, L.; Tomlin, K.; Burke, R.; Westaway, S.M.; Brown, J.A.; Prinjha, R.K.; Martinez, E.D.; Oppermann, U.; Schofield, C.J.; Bountra, C.; Kawamura, A.; Blagg, J.; Brennan, P.E.; Rossanese, O.; Müller, S. Assessing histone demethylase inhibitors in cells: lessons learned. *Epigenetics Chromatin* **2017**, *10*, 9. <http://dx.doi.org/10.1186/s13072-017-0116-6> <https://www.ncbi.nlm.nih.gov/pubmed/28265301>
31. Thinnies, C.C.; England, K.S.; Kawamura, A.; Chowdhury, R.; Schofield, C.J.; Hopkinson, R.J. Targeting histone lysine demethylases - progress, challenges, and the future. *Biochim. Biophys. Acta* **2014**, *1839*(12), 1416-32. <http://dx.doi.org/10.1016/j.bbagr.2014.05.009> <https://www.ncbi.nlm.nih.gov/pubmed/24859458>
32. McAllister, T.E.; England, K.S.; Hopkinson, R.J.; Brennan, P.E.; Kawamura, A.; Schofield, C. Recent Progress in Histone Demethylase Inhibitors. *J Med Chem.* **2016**, *59*(4), 1308-29. <http://dx.doi.org/10.1021/acs.jmedchem.5b01758> <https://www.ncbi.nlm.nih.gov/pubmed/26710088>
33. Itoh, Y.; Sawada, H.; Suzuki, M.; Tojo, T.; Sasaki, R.; Hasegawa, M.; Mizukami, T.; Suzuki, T. Identification of Jumonji AT-Rich Interactive Domain 1A Inhibitors and Their Effect on Cancer Cells. *ACS Med. Chem. Lett.* **2015**, *6*(6), 665-70. <http://dx.doi.org/10.1021/acsmedchemlett.5b00083> <https://www.ncbi.nlm.nih.gov/pubmed/26101571>
34. Gale, M.; Sayegh, J.; Cao, J.; Norcia, M.; Gareiss, P.; Hoyer, D.; Merkel, J.S.; Yan, Q. Screen-identified selective inhibitor of lysine demethylase 5A blocks cancer cell growth and drug resistance. *Oncotarget* **2016**, *7*(26), 39931-39944. <http://dx.doi.org/10.18632/oncotarget.9539> <https://www.ncbi.nlm.nih.gov/pubmed/27224921>
35. Gehling, V.S.; Bellon, S.F.; Harmange, J.C.; LeBlanc, Y.; Poy, F.; Odate, S.; Buker, S.; Lan, F.; Arora, S.; Williamson, K.E.; Sandy, P.; Cummings, R.T.; Bailey, C.M.; Bergeron, L.; Mao, W.; Gustafson, A.; Liu, Y.; VanderPorten, E.; Audia, J.E.; Trojer, P.; Albrecht, B.K. Identification of potent, selective KDM5 inhibitors. *Bioorg. Med. Chem. Lett.* **2016**, *26*(17), 4350-4. <http://dx.doi.org/10.1016/j.bmcl.2016.07.026> <https://www.ncbi.nlm.nih.gov/pubmed/27476424>
36. Mannironi, C.; Proietto, M.; Bufalieri, F.; Cundari, E.; Alagia, A.; Danovska, S.; Rinaldi, T.; Famiglini, V.; Coluccia, A.; La Regina, G.; Silvestri, R.; Negri, R. An high-throughput in vivo screening system to select H3K4-specific histone demethylase inhibitors. *PLoS One.* **2014**, *9*(1). <http://dx.doi.org/10.1371/journal.pone.0086002> <https://www.ncbi.nlm.nih.gov/pubmed/24489688>
37. Kristensen, L.H.; Nielsen, A.L.; Helgstrand, C.; Lees, M.; Cloos, P.; Kastrop, J.S.; Helin, K.; Olsen, L.; Gajhede, M. Studies of H3K4me3 demethylation by KDM5B/Jarid1B/PLU1 reveals strong substrate

- recognition in vitro and identifies 2,4-pyridine-dicarboxylic acid as an in vitro and in cell inhibitor. *FEBS J.* **2012**, 279, 1905-1914. <http://dx.doi.org/10.1111/j.1742-4658.2012.08567.x>  
<https://www.ncbi.nlm.nih.gov/pubmed/22420752>
38. Sayegh, J.; Cao, J.; Zou, M.R.; Morales, A.; Blair, L.P.; Norcia, M.; Hoyer, D.; Tackett, A.J.; Merkel, J.S.; Yan, Q. Identification of small molecule inhibitors of Jumonji AT-rich interactive domain 1B (JARID1B) histone demethylase by a sensitive high throughput screen. *J. Biol. Chem.* **2013**, 288(13), 9408-17. <http://dx.doi.org/10.1074/jbc.M112.419861> <https://www.ncbi.nlm.nih.gov/pubmed/23408432>
  39. Rose, N.R.; Ng, S.; Mecinović, J.; Liénard, B.M.; Bello, S.H.; Sun, Z.; McDonough, M.A.; Oppermann, U.; Schofield, C.J. Inhibitor scaffolds for 2-oxoglutarate-dependent histone lysine demethylases. *J. Med. Chem.* **2008**, 51(22), 7053-6. <http://dx.doi.org/10.1021/jm800936s>  
<https://www.ncbi.nlm.nih.gov/pubmed/18942826>
  40. Luo, X.; Liu, Y.; Kubicek, S.; Myllyharju, J.; Tumber, A.; Ng, S.; Che, K.H.; Podoll, J.; Heightman, T.D.; Oppermann, U.; Schreiber, S.L.; Wang, X. A Selective Inhibitor and Probe of the Cellular Functions of Jumonji C Domain-Containing Histone Demethylases. *J. Am. Chem. Soc.* **2011**, 133, 9451-9456. <http://dx.doi.org/10.1021/ja201597b> <https://www.ncbi.nlm.nih.gov/pubmed/21585201>
  41. Yamamoto, S.; Wu, Z.; Russnes, H.G.; Takagi, S.; Peluffo, G.; Vaske, C.; Zhao, X.; Moen Volla, H.K.; Maruyama, R.; Ekram, M.B.; Sun, H.; Kim, J.H.; Carver, K.; Zucca, M.; Feng, J.; Almendro, V.; Bessarabova, M.; Rueda, O.M.; Nikolsky, Y.; Caldas, C.; Liu, X.S.; Polyak, K. *Cancer Cell.* **2014**, 25(6), 762-77. <http://dx.doi.org/10.1016/j.ccr.2014.04.024> <https://www.ncbi.nlm.nih.gov/pubmed/24937458>
  42. Kim, S.; Dere, E.; Burgoon, L.D.; Chang, C.C.; Zacharewski, T.R. Comparative analysis of AhR-mediated TCDD-elicited gene expression in human liver adult stem cells. *Toxicol. Sci.* **2009**, 112(1), 229-44. <http://dx.doi.org/10.1093/toxsci/kfp189> <https://www.ncbi.nlm.nih.gov/pubmed/19684285>
  43. Lee, H.H.; Kim, W.T.; Kim, D.H.; Park, J.W.; Kang, T.H.; Chung, J.W.; Leem, S.H. Tristetraprolin suppresses AHR expression through mRNA destabilization. *FEBS Lett.* **2013**, 587(10), 1518-23. <http://dx.doi.org/10.1016/j.febslet.2013.03.031> <https://www.ncbi.nlm.nih.gov/pubmed/23583445>
  44. MacPherson, L.; Ahmed, S.; Tamblyn, L.; Krutmann, J.; Förster, I.; Weighardt, H.; Matthews, J. Aryl hydrocarbon receptor repressor and TipARP (ARTD14) use similar, but also distinct mechanisms to repress aryl hydrocarbon receptor signaling. *Int. J. Mol. Sci.* **2014**, 15(5), 7939-57. <http://dx.doi.org/10.3390/ijms15057939> <https://www.ncbi.nlm.nih.gov/pubmed/24806346>
  45. Kanno, Y.; Takane, Y.; Izawa, T.; Nakahama, T.; Inouye, Y. The inhibitory effect of aryl hydrocarbon receptor repressor (AhRR) on the growth of human breast cancer MCF-7 cells. *Biol. Pharm. Bull.* **2006**, 29(6), 1254-7. <https://www.ncbi.nlm.nih.gov/pubmed/16755028> <https://doi.org/10.1248/bpb.29.1254>
  46. Srikannathasan, V.; Wohlfonig, A.; Shillings, A.; Singh, O.; Chan, P.F.; Huang, J.; Gwynn, M.N.; Fosberry, A.P.; Homes, P.; Hibbs, M.; Theobald, A.J.; Spitzfaden, C.; Bax, B.D. Crystallization and initial crystallographic analysis of covalent DNA-cleavage complexes of *Staphylococcus aureus* DNA gyrase with QPT-1, moxifloxacin and etoposide. *Acta Crystallogr F Struct Biol Commun.* **2015**, 71, 1242-6. <https://doi.org/10.1107/S2053230X15015290> <https://www.ncbi.nlm.nih.gov/pubmed/26457513>
  47. Bavetsias, V.; Lanigan, R.M.; Ruda, G.F.; Atrash, B.; McLaughlin, M.G.; Tumber, A.; Mok, N.Y.; Le Bihan, Y.V.; Dempster, S.; Boxall, K.J.; Jegannathan, F.; Hatch, S.B.; Savitsky, P.; Velupillai, S.; Krojer, T.; England, K.S.; Sejberg, J.; Thai, C.; Donovan, A.; Pal, A.; Scozzafava, G.; Bennett, J.M.; Kawamura, A.; Johansson, C.; Szykowska, A.; Gileadi, C.; Burgess-Brown, N.A.; von Delft, F.; Oppermann, U.; Walters, Z.; Shipley, J.; Raynaud, F.I.; Westaway, S.M.; Prinjha, R.K.; Fedorov, O.; Burke, R.; Schofield, C.J.; Westwood, I.M.; Bountra, C.; Müller, S.; van Montfort, R.L.; Brennan, P.E.; Blagg, J. 1,8-Substituted Pyrido[3,4-D]Pyrimidin-4(3H)-One Derivatives as Potent, Cell Permeable, Kdm4 (Jmjd2) and Kdm5 (Jarid1) Histone Lysine Demethylase Inhibitors. *J. Med. Chem.* **2016**, 59, 1388-1409, <https://doi.org/10.1021/acs.jmedchem.5b01635> <https://www.ncbi.nlm.nih.gov/pubmed/26741168>
  48. Tumber, A.; Nuzzi, A.; Hookway, E.S.; Hatch, S.B.; Velupillai, S.; Johansson, C.; Kawamura, A.; Savitsky, P.; Yapp, C.; Szykowska, A.; Wu, N.; Bountra, C.; Strain-Damerell, C.; Burgess-Brown, N.A.; Ruda, G.F.; Fedorov, O.; Munro, S.; England, K.S.; Nowak, R.P.; Schofield, C.J.; La Thangue, N.B.; Pawlyn, C.; Davies, F.; Morgan, G.; Athanasou, N.; Müller, S.; Oppermann, U.; Brennan, P.E. Potent and Selective KDM5 Inhibitor Stops Cellular Demethylation of H3K4me3 at Transcription Start Sites and Proliferation of MM1S Myeloma Cells. *Cell. Chem. Biol.* **2017**, 24(3):371-380. <http://dx.doi.org/10.1016/j.chembiol.2017.02.006>  
<https://www.ncbi.nlm.nih.gov/pubmed/28262558>

49. Scibetta, A.G.; Santangelo, S.; Coleman, J.; Hall, D.; Chaplin, T.; Copier, J.; Catchpole, S.; Burchell, J.N.; Taylor-Papadimitriou, J. Functional analysis of the transcription repressor PLU-1/JARID1B. *Mol. Cell. Biol.* **2007**, *27*(20), 7220-35. <http://dx.doi.org/10.1128/MCB.00274-07> <https://www.ncbi.nlm.nih.gov/pubmed/17709396>
50. Wenners, A.; Hartmann, F.; Jochens, A.; Roemer, A.M.; Alkatout, I.; Klapper, W.; van Mackelenbergh, M.; Mundhenke, C.; Jonat, W.; Bauer, M. Stromal markers AKR1C1 and AKR1C2 are prognostic factors in primary human breast cancer. *Int. J. Clin. Oncol.* **2016**, *21*(3), 548-56. <http://dx.doi.org/10.1007/s10147-015-0924-2> <https://www.ncbi.nlm.nih.gov/pubmed/26573806>
51. Ying, J.; Li, H.; Seng, T.J.; Langford, C.; Srivastava, G.; Tsao, S.W.; Putti, T.; Murray, P.; Chan, A.T.; Tao, Q. Functional epigenetics identifies a protocadherin PCDH10 as a candidate tumor suppressor for nasopharyngeal, esophageal and multiple other carcinomas with frequent methylation. *Oncogene* **2006**, *25*(7), 1070-80. <http://dx.doi.org/10.1038/sj.onc.1209154> <https://www.ncbi.nlm.nih.gov/pubmed/16247458>
52. Penterling, C.; Drexler, G.A.; Böhlend, C.; Stamp, R.; Wilke, C.; Braselmann, H.; Caldwell, R.B.; Reindl, J.; Girst, S.; Greubel, C.; Siebenwirth, C.; Mansour, W.Y.; Borgmann, K.; Dollinger, G.; Unger, K.; Friedl, A.A. Depletion of Histone Demethylase Jarid1A Resulting in Histone Hyperacetylation and Radiation Sensitivity Does Not Affect DNA Double-Strand Break Repair. *PLoS One* **2016**, *11*(6). <http://dx.doi.org/10.1371/journal.pone.0156599> <https://www.ncbi.nlm.nih.gov/pubmed/27253695>
53. Rafehi, H.; Orlowski, C.; Georgiadis, G.T.; Ververis, K.; El-Osta, A.; Karagiannis, T.C. Clonogenic assay: adherent cells. *J. Vis. Exp.* **2011**, 49. <http://dx.doi.org/10.3791/2573> <https://www.ncbi.nlm.nih.gov/pubmed/1445039>
54. Ding, D.; Zhang, Y.; Wang, J.; Wang, X.; Fan, D.; He, L.; Zhang, X.; Gao, Y.; Li, Q.; Chen, H.  $\gamma$ -H2AX/53BP1/pKAP-1 foci and their linear tracks induced by in vitro exposure to radon and its progeny in human peripheral blood lymphocytes. *Sci Rep.* **2016**, *6*, 38295. <http://dx.doi.org/10.1038/srep38295> <https://www.ncbi.nlm.nih.gov/pubmed/27922110>
55. Dimitrova, E.; Turberfield, A.H.; Klose, R.J. Histone demethylases in chromatin biology and beyond. *EMBO Rep.* **2015**, *16*, 1620-1639. <http://dx.doi.org/10.15252/embr.201541113> <https://www.ncbi.nlm.nih.gov/pubmed/26564907>
56. Rath, B.H.; Waung, I.; Camphausen, K.; Tofilon, P.J. Inhibition of the histone H3K27 demethylase UTX enhances tumor cell radiosensitivity. *Mol Cancer Ther.* **2018**, *17*(5), 1070-1078. <http://dx.doi.org/10.1158/1535-7163.MCT-17-1053> <https://www.ncbi.nlm.nih.gov/pubmed/29483212>
57. Trapnell, C.; Roberts, A.; Goff, L.; Pertea, G.; Kim, D.; Kelley, D.R.; Pimentel, H.; Salzberg, S.L.; Rinn, J.L.; Pachter, L. Differential gene and transcript expression analysis of RNA-seq experiments with TopHat and Cufflinks. *Nat. Protoc.* **2012**, *7*, 562-578. <http://dx.doi.org/10.1038/nprot.2012.016> <https://www.ncbi.nlm.nih.gov/pubmed/22383036>
58. Gentleman, R.C.; Carey, V.J.; Bates, D.M.; Bolstad, B.; Dettling, M.; Dudoit, S.; Ellis, B.; Gautier, L.; Ge, Y.; Gentry, J.; Hornik, K.; Hothorn, T.; Huber, W.; Iacus, S.; Irizarry, R.; Leisch, F.; Li, C.; Maechler, M.; Rossini, A.J.; Sawitzki, G.; Smith, C.; Smyth, G.; Tierney, L.; Yang, J.Y.; Zhang, J. Bioconductor: open software development for computational biology and bioinformatics. *Genome Biol.* **2004**, *5*, R80. <http://dx.doi.org/10.1186/gb-2004-5-10-r80> <https://www.ncbi.nlm.nih.gov/pubmed/15461798>
59. Yu, G.; Wang, L.G.; Han, Y.; He, Q.Y. clusterProfiler: an R Package for Comparing Biological Themes Among Gene Clusters. *OMICS J. Integr. Biol.* **2012**, *16*, 284-287. <http://dx.doi.org/10.1089/omi.2011.0118> <https://www.ncbi.nlm.nih.gov/pubmed/22455463>
60. Ashburner, M.; Ball, C.A.; Blake, J.A.; Botstein, D.; Butler, H.; Cherry J.M.; Davis, A.P.; Dolinski, K.; Dwight, S.S.; Eppig, J.T.; Harris, M.A.; Hill, D.P.; Issel-Tarver, L.; Kasarskis, A.; Lewis, S.; Matese, J.C.; Richardson, J.E.; Ringwald, M.; Rubin, G.M.; Sherlock, G. Gene Ontology: tool for the unification of biology. *Nat. Genet.* **2000**, *25*, 25-29. <http://dx.doi.org/10.1038/75556> <https://www.ncbi.nlm.nih.gov/pubmed/10802651>
61. Ilari, A.; Fiorillo, A.; Poser, E.; Lalioti, V.S.; Sundell, G.N.; Ivarsson, Y.; Genovese, I.; Colotti, G. Structural basis of Sorcin-mediated calcium-dependent signal transduction. *Sci Rep.* **2015**, *5*:16828. <http://dx.doi.org/10.1038/srep16828> <https://www.ncbi.nlm.nih.gov/pubmed/26577048>
62. Sastry, G.M.; Adzhigirey, M.; Day, T.; Annabhimoju, R.; Sherman, W. Protein and ligand preparation: parameters, protocols, and influence on virtual screening enrichments. *J Comput Aided Mol Des.* **2013**, *3*, 221-34 <http://dx.doi.org/10.1007/s10822-013-9644-8> <https://www.ncbi.nlm.nih.gov/pubmed/23579614>

63. Korb, O.; Stützle, T.; Exner, T.E. Empirical scoring functions for advanced protein-ligand docking with PLANTS. *J. Chem. Inf. Model.* **2009**, *49* (1), 84–96. <http://dx.doi.org/19125657>  
<https://www.ncbi.nlm.nih.gov/pubmed/10.1021/ci800298z>
64. Shechter, D.; Dormann, H.L.; Allis, C.D.; Hake, S.B. Extraction, purification and analysis of histones. *Nat. Protoc.* **2007**, *2*(6), 1445-57. <http://dx.doi.org/10.1038/nprot.2007.202>  
<https://www.ncbi.nlm.nih.gov/pubmed/17545981>
65. Livak, K.J.; Schmittgen, T.D. Analysis of relative gene expression data using real-time quantitative PCR and the 2(-Delta Delta C(T)) Method. *Methods* **2001**, *25*(4), 402-8. <http://dx.doi.org/10.1006/meth.2001.1262>  
<https://www.ncbi.nlm.nih.gov/pubmed/11846609>
66. Schindelin, J.; Arganda-Carreras, I.; Frise, E.; Kaynig, V.; Longair, M.; Pietzsch, T.; Preibisch, S.; Rueden, C.; Saalfeld, S.; Schmid, B.; Tinevez, J.Y.; White, D.J.; Hartenstein, V.; Eliceiri, K.; Tomancak, P.; Cardona, A. Fiji: An Open-Source Platform for Biological-Image Analysis. *Nat. Methods* **2012**, *9*(7), 676-82. <http://dx.doi.org/10.1038/nmeth.2019> <https://www.ncbi.nlm.nih.gov/pubmed/22743772>